3. Results

3.1. FLV + TBI treatment leads to an overexpression of downstream molecules of p in the bone marrow of C3H mice

To address the molecular basis for the *p53*-dependent apoptosis in FLV + TBI-treated C3H mice, downstream molecules of *p53* signaling were analyzed in bone marrow cells using the RT-PCR technique. As expected from the previous observation that p53 was stabilized and accumulated in response to genotoxic stress [1–3], mRNA levels for *p21* and *bax*, both of which were *p53*-target genes, exhibited overexpression after treatment with TBI alone (Fig. 1). However, bone marrow cells from FLV + TBI-treated C3H mice exhibited a much greater expression of *p21* as well as *bax*, in spite that the expression of *β-actin* mRNA was a little weaker in FLV + TBI-treated sample. These results suggested that genes encoding downstream molecules of *p53* would be widely upregulated after FLV + TBI-treatment.

3.2. SCID mice and ATM knockout mice with the C3H background are refractory to the apoptosis enhanced by FLV + TBI treatment

To investigate the role of upstream molecules of p53, PI3 kinases, in FLV + TBI treatment, DNA-PK-deficient SCID mice and *ATM* knockout mice with the C3H background were analyzed. First, apoptotic cells of the bone marrow were identified using the TUNEL method (Fig. 2A). When mice were treated with TBI alone, apoptotic cells were more significantly frequent in the bone marrow of C3H·SCID (9.5 ± 0.9%, mean ± S.E.M.) than wild type C3H (6.1 ± 0.7%) at 3 h ($p < 0.01$, Student's *t*-test). These findings were consistent with the previous findings that SCID mice and cells are hypersensitive to ionizing irradiation [17]. Conversely, bone marrow cells of C3H $ATM^{-/-}$ mice exhibited significantly lower percentages of apoptotic cells (2.8 ± 0.2%) than those of wild type C3H mice ($p < 0.001$). In wild type C3H mice, apoptotic bone marrow cells were much more frequent in FLV + TBI-treated mice as compared with TBI-treated mice (Fig. 2A). Although the data are not shown, apoptotic cells before 3 h after FLV + TBI were fewer than those at 3 h. Thus, the peak apoptosis was observed at 3 h after FLV + TBI-treatment. However, in C3H·SCID and $ATM^{-/-}$ mice, the frequency of apoptotic cells after FLV + TBI treatment was similar to that after TBI-alone treatment. Thus, the enhancing effect of FLV infection on irradiation-induced apoptosis appeared negative in the bone marrow of C3H·SCID and $ATM^{-/-}$ mice. Although the data is not shown, gp70 protein levels of bone marrow cells were similar in wild, SCID, and $ATM^{-/-}$ mice after infection with FLV. Fig. 2B shows the actual figures of TUNEL reaction in the bone marrow of wild C3H mice with sham-treatment (a), TBI alone (b), and FLV + TBI treatment (c).

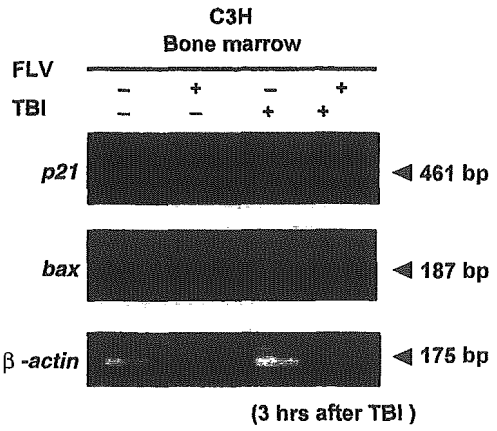

Fig. 1. RT-PCR analysis for the expression of *p21* and *bax* mRNA in the bone marrow of C3H mice. RNA samples were prepared from the bone marrow of untreated, FLV-treated, TBI-treated, and FLV + TBI-treated C3H mice 3 h after TBI treatment (+, present; –, absent). Although TBI-treatment induced a slight increase in the expression of *p21* and *bax* mRNA, FLV + TBI-treatment induced a remarkable increase of *p21* and *bax* expression.

3.3. p53 is accumulated and phosphorylated in the bone marrow of C3H mice after FLV + TBI treatment but not in SCID and ATM knockout mice

Next, bone marrow cell lysate was immunoprecipitated with anti-p53 antibody and then, the precipitate was analyzed for p53 phosphorylated at Ser-18 by immunoblotting. As shown in Fig. 3, TBI-treated mice exhibited a slight increase in intensity of the phosphorylated p53 signal 3 h after TBI with a return to the control level by 12 h. By contrast, phosphorylation was prominent in bone marrow cells from FLV + TBI-treated C3H mice 3 and 12 h after TBI. Although FLV-infection alone caused weak signals of p53 accumulation and phosphorylation (FLV (+), 0 h), this may be associated with the fact that retroviral integration to the host DNA would be recognized as a mild DNA damage by the host cells [38]. Concerning the discrepancy between the timing of apoptosis as measured by TUNEL assay and the activation of the p53 pathway in FLV + TBI-treated C3H mice, several comments may have to be added. Although we could observe the peak of apoptosis at 3 h after FLV + TBI, the reaction might actually continue even after this period. Because the macrophage-lineage cells should be activated and eliminate these apoptotic cells thereafter by phagocytosis and thus, the number of apoptotic figures may represent the balance of apoptosis and the activity of cells with phagocytosis. We might be able to detect the increased or peak apoptosis before the activation of macrophage-lineage cells occur. Therefore, we might detect the p53 activation still at 12 h after FLV + TBI. Actual apoptosis may continuously be induced because the in vivo experiments revealed remarkable loss of bone marrow hematopoietic cells in due course resulting in almost depletion by 20 days after FLV + TBI treatment.

As shown in Fig. 3, bone marrow cells of TBI-treated SCID mice exhibited p53 accumulation and phosphoryla-

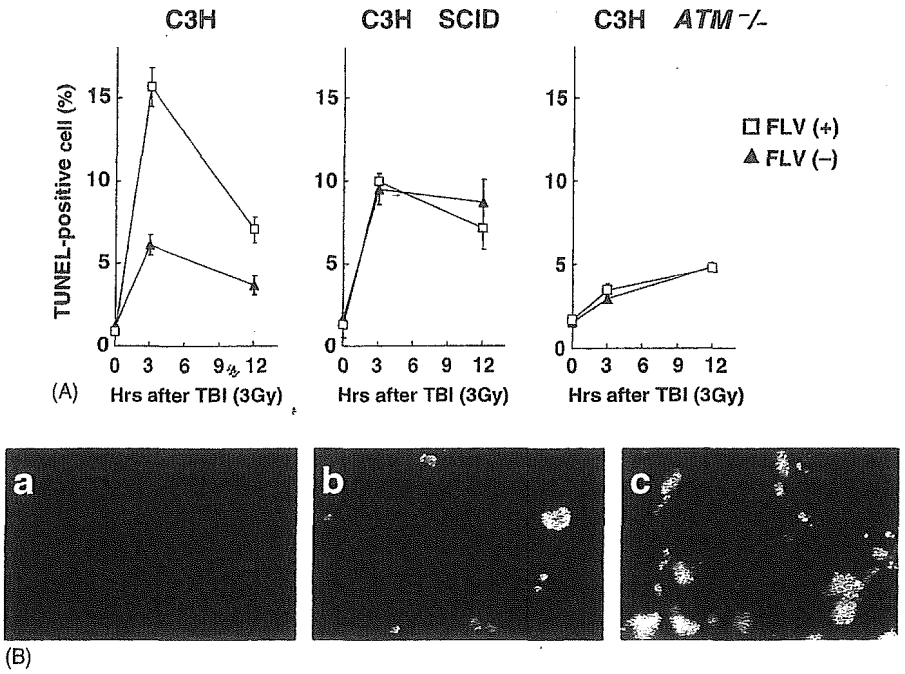

Fig. 2. (A) Apoptotic cell ratio and p53 status in the bone marrow of wild type, SCID, and $ATM^{-/-}$ mice with the C3H background after treatment with FLV and/or TBI. The TUNEL-positive cell ratio of bone marrow cells from FLV (−) or FLV (+) C3H wild type, C3H·SCID, and C3H·$ATM^{-/-}$ mice after treatment with TBI (3 Gy). Error bars indicate standard errors of the means calculated from the data from three to five mice at each point. C3H wild type mice exhibited a prominent increase in the ratio of TUNEL-positive cells with a peak at 3 h after TBI treatment, however in SCID and $ATM^{-/-}$ mice, the frequency of TUNEL-positive cells in FLV-infected mice was similar to that in FLV (−) mice after TBI treatment. (B) Apoptotic cells in the bone marrow of TBI-treated or FLV + TBI-treated mice with the C3H background. TUNEL staining of bone marrow specimens from a sham-treated control mouse (a), TBI-treated mouse (b), and FLV + TBI-treated mouse (c). Bone marrow samples were isolated at 3 h after TBI (3 Gy)-treatment and stained for apoptotic cells (original magnification, 130×). Note the many TUNEL-positive cells in the FLV + TBI-treated C3H mouse in contrast to the TBI alone-treated mouse.

tion, whereas TBI-treated $ATM^{-/-}$ mice showed almost no signal for p53 and phospho-p53 protein. After FLV + TBI-treatment, the expression of p53 and phospho-p53 protein did not show a remarkable increase in the bone marrow cells of either mice. These results indicated that ATM was required for the activation of p53 in response to TBI alone, but DNA-PK as well as ATM was required for enhanced p53 activation in C3H bone marrow cells after treatment with FLV + TBI.

3.4. *DNA-PK is overexpressed after treatment with FLV + TBI*

To determine the expression dynamics of DNA-PK and ATM after TBI treatment at the protein level, immunoblotting was performed using whole lysate from C3H bone marrow cells. In FLV-free (−) mice, DNA-PK expression seemed stable after TBI treatment, however, FLV-infected (+) mice exhibited a prominent increase of DNA-PK expression after the treatment (Fig. 4A). In contrast, the expression of ATM was slightly up-regulated both in FLV (−) and FLV (+) mice peaking at 3 h after TBI, although the pattern of dynamics and the intensity of bands were similar in the FLV (−) and FLV (+) conditions. ATM usually introduces *p53*-dependent apoptosis after TBI treatment. We interpreted the role of ATM in FLV + TBI-treatment as the trigger for elevating the basic level of p53-activation by TBI. Therefore, the kinetics of ATM protein expression appeared equivalent in mice regardless of FLV infection. In contrast, DNA-PK may not be essential for DNA-damage-induced apoptosis itself because SCID mice exhibited certain level of apoptosis after TBI-treatment as shown in Fig. 2A, but would be important for additional activation of p53 by FLV-infection.

Next, to test whether the overexpression of DNA-PK protein is correlated with the expression at the mRNA level, RT-PCR assays were performed for *DNA-PK* and *ATM* mRNA in each experimental group. As shown in Fig. 4B, the mRNA expression of *DNA-PK* and *ATM* appeared rather stable after treatment with FLV, TBI or FLV + TBI, although *ATM* expression was slightly enhanced by FLV-infection. These results in Fig. 4A and B suggested that mechanisms such as post-transcriptional regulation might control the protein levels of these PI3 kinases in TBI- or FLV + TBI-treated mice. Further study should clarify the discrepancy of *DNA-PK/ATM* expression at the protein level and the mRNA level.

3.5. *DNA-PK and ATM demonstrate enhanced kinase activity after treatment with FLV + TBI*

To confirm whether DNA-PK or ATM in the bone marrow cells of C3H mice treated with FLV + TBI actually

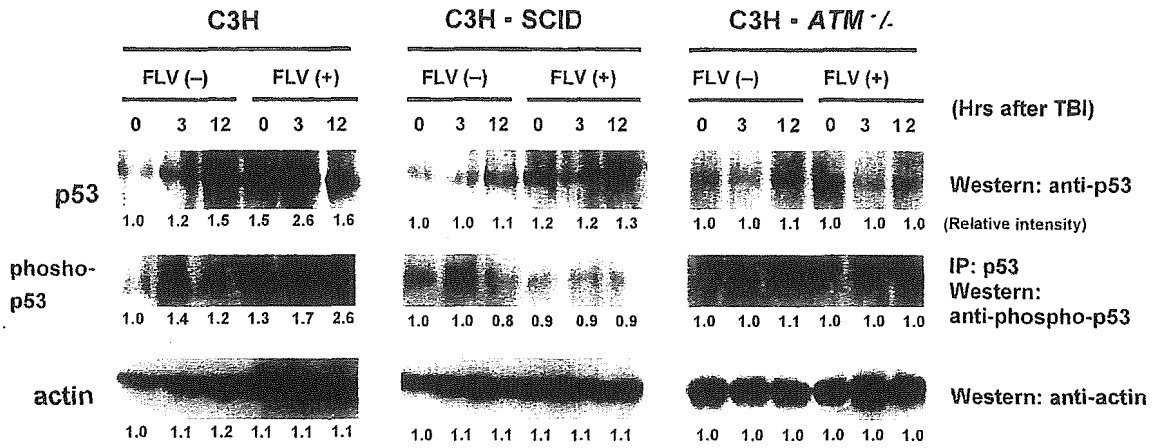

Fig. 3. Immunoblotting for p53 protein and phospho-p53 protein in bone marrow from C3H wild type, C3H·SCID, and C3H·$ATM^{-/-}$ mice 0, 3, and 12 h after TBI treatment (3 Gy). Cell lysates were prepared from the bone marrow of FLV (–) or FLV (+) C3H wild type, C3H·SCID, and C3H·$ATM^{-/-}$ mice. As the bands for actin protein exhibited a similar density in each sample, the amount of protein contained in cell lysates is similar in each lane. The relative intensities of bands were measured by densitometry (FLV (–), 0 h as the control, 1.0) and indicated under the photos of gels. C3H wild type mice revealed marked overexpression of p53 protein as well as phopspho-p53 when treated with FLV + TBI, although TBI alone also induced a slight increase of p53 and phopspho-p53 expression. By contrast, SCID and $ATM^{-/-}$ mice exhibited similar levels of p53 protein and phospho-p53 protein expression in the bone marrow samples of FLV (–) mice and FLV (+) mice after TBI-treatment.

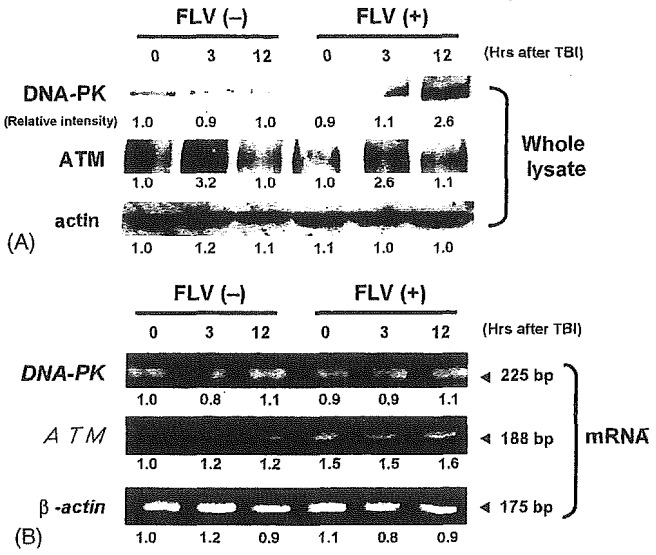

Fig. 4. (A) Immunoblotting for DNA-PK and ATM protein in the bone marrow of C3H mice 0, 3, and 12 h after TBI (3 Gy). Cell lysate (100 μg) from the bone marrow of FLV (–) or FLV (+) C3H mice was used for this assay. Actin protein levels of each sample are shown to confirm that the amounts of samples loaded were almost equal. The relative intensities of bands were measured by densitometry (FLV (–), 0 h as the control, 1.0) and indicated under the photos of gels. Note that DNA-PK protein levels were remarkably higher in the bone marrow from FLV (+) C3H mice 3 and 12 h after TBI than the FLV-treated (0 h) mice. By contrast, DNA-PK protein levels of FLV (–) C3H samples exhibited no remarkable change. ATM protein levels were enhanced by TBI-treatment but not enhanced by FLV-infection. (B) RT-PCR analysis for mRNA of *DNA-PK* and *ATM* in the bone marrow of C3H mice 0, 3, and 12 h after TBI treatment (3 Gy). The expression of *β-actin* mRNA levels of each sample was similar. The relative intensities of bands were measured by densitometry (FLV (–), 0 h as the control, 1.0) and indicated under the photos of gels. Note that changes in mRNA expression for *DNA-PK* as well as *ATM* were not remarkable between samples from each group although *ATM* expression exhibited slight increase in FLV (+) samples.

phosphorylated the p53 protein, kinase assays of DNA-PK and ATM were performed using bone marrow cells of FLV (–) and FLV (+) C3H mice treated with TBI. As DNA-PK and ATM can phosphorylate Ser-15 of p53 protein in vitro [10,12,13,39], immunoprecipitates obtained with anti-DNA-PK or anti-ATM antibody using protein extracts of bone marrow cells were mixed with exogeneous p53 protein as the substrate. Then, the phosphorylation of p53 was determined by immunoblotting with anti-phospho-p53 Ser-15 antibody (also reacted with murine Ser-18 of phospho-p53) to evaluate the DNA-PK/ATM kinase activity (Fig. 5). The differences in p53 phosphorylation levels may probably be influenced by the unequal presence of immunoprecipitated kinases (DNA-PK or ATM) as shown in Fig. 4A.

The DNA-PK activity was at the control level after treatment with TBI alone, while FLV + TBI evoked a high level of DNA-PK activity in C3H mice. In the ATM kinase assay, the phospho-p53 band exhibited a higher level in mice treated with TBI alone than in control mice. Further, the ATM kinase activity of bone marrow cells from FLV + TBI-treated C3H mice was only slightly stronger than that of TBI-treated mice. Both of DNA-PK and ATM kinase activities were slightly up-regulate by FLV alone-treatment (FLV (+), 0 h). These signals might correspond to the mild DNA damage signals by retroviral integration to the host cells [38]. As negative controls, immunoprecipitates obtained with anti-DNA-PK or anti-ATM antibody that were not mixed with exogenous p53 protein were also examined for Ser-18 phospho-p53 and exhibited negative signals (data not shown). These results suggested that TBI-treatment activated ATM kinase but not DNA-PK, although FLV + TBI treatment enhanced the ability of DNA-PK in addition to the ATM kinase to activate p53.

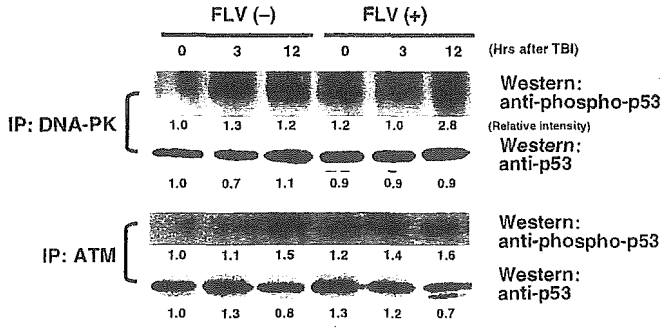

Fig. 5. Kinase assays for DNA-PK and ATM from the bone marrow of C3H mice 0, 3, and 12 h after TBI (3 Gy). Cell extracts were prepared from the bone marrow of FLV (−) or FLV (+) C3H mice. Immunoprecipitates for DNA-PK or ATM were prepared by mixing equal amount of lysate with anti-DNA-PK or ATM antibody. The kinase activity of each immunoprecipitate which would phosphorylate recombinant human p53 protein at Ser 15 in vitro was assessed by immunoblotting for phospho-p53 protein. The relative intensities of bands were measured by densitometry (FLV (−), 0 h as the control, 1.0) and indicated under the photos of gels. The same samples after the kinase reaction were also assayed for the amount of total p53 protein by immunoblotting. Note the prominent signals for phospho-p53 in FLV + TBI-treated mice at 12 h in the DNA-PK immunoprecipitate. By contrast, ATM immunoprecipitates from FLV (−) and FLV (+) mice exhibited a similar enhancement of phospho-p53 signals at 12 h after TBI, although FLV (+) mice exhibited a little stronger signal than FLV (−) mice. The total amount of p53 protein in the DNA-PK immunoprecipitates and ATM immunoprecipitates was similar in each experimental group.

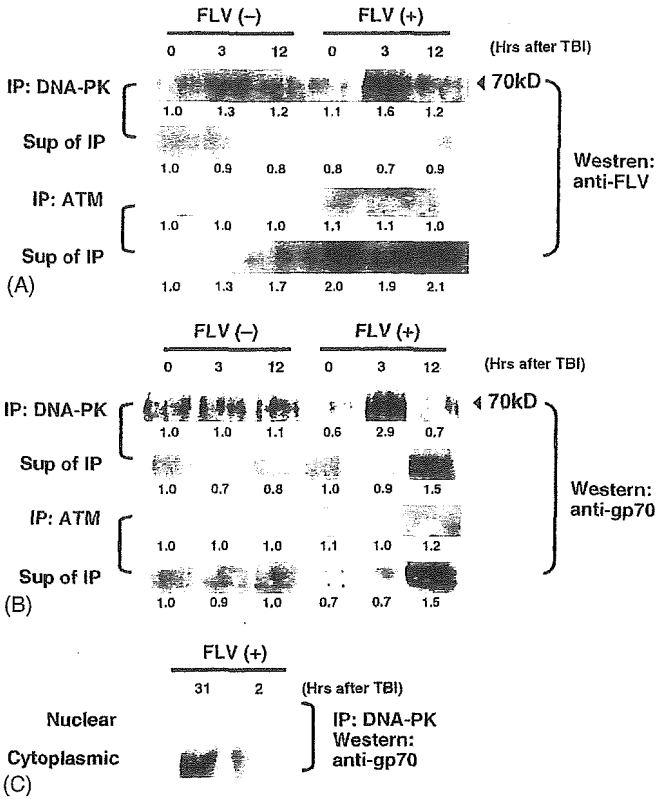

Fig. 6. (A) Co-immunoprecipitation analysis for DNA-PK or ATM with FLV-associated protein detected by anti-Friend MuLV antibody in the bone marrow of C3H mice 0, 3, and 12 h after TBI treatment (3 Gy). Cell lysate from bone marrow of FLV (−) or FLV (+) C3H mice was immunoprecipitated with anti-DNA-PK or anti-ATM antibody, then the immunoprecipitates were immunoblotted using antibody against Friend MuLV which is known to cross-react with FLV-associated proteins. Supernatants of the immnoprecipitates were also immunoblotted for FLV-associated proteins. The FLV-associated proteins were strongly co-immunoprecipitated with DNA-PK in the bone marrow of FLV (+) C3H mice 3 h after TBI at the size circa 70 kD, whereas no co-immunoprecipitation of viral protein with ATM was detected in any samples. Although the viral protein was also detected in FLV (−) mice, these weak signals would indicate the cross-reaction of this antibody with endogenous viral proteins. (B) A similar experiment using anti-Moloney MuLV gp70 antibody which is known to cross-react with Friend MuLV gp70. Note that gp70 was strongly co-immunoprecipitated with DNA-PK in the bone marrow of FLV + TBI-treated C3H mice. The relative intensities of bands were measured by densitometry (FLV (−), 0 h as the control, 1.0) and indicated under the photos of gels. (C) Co-immunoprecipitation analysis for DNA-PK with gp70 using fractionated cell lysate of the bone marrow from FLV-infected C3H mice 3 and 12 h after TBI treatment (3 Gy). Nuclear fraction and cytoplasmic fraction of cell lysate were prepared from FLV + TBI-treated mice and then, the immunoprecipitates with anti-DNA-PK antibody were immunoblotted using antibody against Moloney MuLV gp70. Note the positive signals in the cytoplasmic fraction of lysate from FLV + TBI-treated mice.

3.6. DNA-PK interacts with gp70 in response to FLV + TBI-treatment

As FLV enhances apoptosis and p53 activation in DNA damage-induced signaling pathways, an FLV-specific molecule might be involved in the activation of p53. Thus, to examine the interactions between p53 protein, DNA-PK, ATM, and the FLV-specific molecule, lysates from C3H bone marrow cells were immunoprecipitated with anti-DNA-PK or anti-ATM antibody and then, the precipitates were immunoblotted for FLV-associated proteins using polyclonal antibody against FLV-associated proteins. As shown in Fig. 6A, protein with circa 70 kD size appeared strongly co-precipitated with DNA-PK in the bone marrow cells of FLV-infected C3H mice (3 h after TBI treatment). When supernatants of DNA-PK immunoprecipitates were immunoblotted for FLV-associated proteins, we could confirm that bands for the same protein (about 70 kD in size) were relatively stronger in samples 0 and 12 h after TBI than in the sample 3 h after TBI. In contrast, immunoprecipitates obtained with anti-ATM antibody did not exhibit any positive bands for FLV-associated proteins (Fig. 6A). Because we could detect the viral protein with the molecular size around 70 kD, further to confirm the specificity of interaction of DNA-PK with gp70, which is known as a F-MuLV env protein [40], similar experiments were performed using anti-Moloney MuLV gp70 antibody and anti-Raucher MuLV gp70 antibody. As shown in Fig. 6B (only the Moloney MuLV gp70 data are shown because the data were basically identical), viral protein with the molecular size of about 70 kD was co-precipitated with DNA-PK but not with ATM in FLV + TBI-treated mice, although it is still unclear whether the interaction was direct or indirect. Taken together with the data from Fig. 4A, DNA-PK was accumulated (peaked at 12 h) after strong interaction with gp70 (peaked at 3 h) in FLV + TBI-treated C3H bone marrow cells. These findings would suggest that

the increase in the amount of DNA-PK might be related to the interaction between DNA-PK and gp70. Co-precipitation was not demonstrated between p53 and DNA-PK, p53 and ATM, or p53 and gp70 (data not shown). To determine whether the interaction occur in the cytoplasm or nucleus of FLV-infected cells, fractionated lysate was analyzed for co-precipitation of gp70 with DNA-PK. As shown in Fig. 6C, gp70 was mainly co-precipitated with DNA-PK in the cytoplasmic fraction of cell lysate from FLV + TBI treated mice.

4. Discussion

Ionizing irradiation induces a marked increase in cellular p53 protein followed by the consequent transmission of DNA damage signals [1]. The prominent apoptosis induced by FLV + TBI-treatment in the present study was *p53*-dependent, although the apoptosis observed in liquid-cultured FLV-induced primary erythroleukemic cells has been reported to be *p53*-independent [41]. As expected, expression of the *p53* target molecule, *bax*, was up-regulated, however, *p21* which has a role in cell cycle arrest signaling was also overexpressed. These findings suggested that FLV + TBI treatment induced p53 activation leading to not only apoptosis but also other DNA damage responses. Therefore, key molecules modifying the transcriptional activity of *p53* might be located upstream of p53 in the signaling pathway of this model.

In response to DNA-double strand breaks, candidates for the upstream activators of p53 would include two members of the PI3 kinase family, ATM and DNA-PK. ATM phosphorylates p53 in vivo [13], while DNA-PK has been proved to phosphorylate p53 in in vitro systems but not in in vivo systems [9]. Using mouse embryonic fibroblasts lacking DNA-PK, Jimenez et al. [15] have demonstrated that DNA-PK was not required for the p53-dependent response to DNA damage. However, our results demonstrated that not only ATM but also DNA-PK played an important role in inducing a lethal apoptosis in FLV + TBI-treated mice in vivo, whereas only ATM but not DNA-PK was required for the mild apoptotic response after low-dose TBI in bone marrow cells of C3H mice. The result suggested that FLV infection modifies the innate signaling pathway of C3H bone marrow cells to activate p53 after irradiation.

We report here that FLV-infection actually modifies the DNA-PK molecule after treatment with TBI. gp70, known as an env protein of F-MuLV, strongly interacted with DNA-PK. The interaction was mainly observed in the cytoplasmic fraction of FLV-infected cell lysate suggesting that DNA-PK with gp70 complex would be formed in the cytoplasm and then, function as a kinase and activate *p53* signaling. DNA-PK is known to associate with various proteins including Ku, which stimulates the catalytic subunit of DNA-PK (DNA-PKcs) leading to effective V(D)J recombination and DNA double-strand break repair in vivo [17,42]. Although other factors would be involved in the interaction between DNA-PK and gp70, gp70 might act as an enhancing factor for DNA-PK to be immediately accumulated and also in kinase activity to phosphorylate p53.

It remains unclear how DNA-PK or ATM works in DNA damage-induced signaling to activate p53 in FLV-infected C3H cells. Shangary et al. [37] demonstrated that ATM activated c-Abl kinase in response to ionizing irradiation and subsequently the activated c-Abl regulated DNA-PK activity in vivo. Thus, in the present experimental system also, DNA-PK and ATM might cooperate through other factors such as c-Abl kinase. Another possibility would be that DNA-PK and ATM separately activate p53 protein on FLV + TBI-treatment. The functional complementation of these two molecules was demonstrated by the fact that mice deficient in both DNA-PK (SCID mutation) and ATM show embryonic lethality [43]. In addition, the function of DNA-PK in non-homologous end joining (NHEJ) would partly be performed by ATM [38,44]. These results suggest that DNA-PK and ATM should have similar and sometimes complementary roles in various cellular pathways.

Recently, Woo et al. [45] have shown that DNA-PKcs forms a complex with latent p53 immediately following γ-irradiation, and latent murine p53 phosphorylated at Ser-18 by DNA-PK is required for DNA damage-induced apoptosis. In our experimental system, bone marrow cells from C3H-SCID mice exhibited positive signals for p53 activation and an apoptotic response when treated with TBI alone, but did not exhibit enhanced signals when treated with FLV + TBI. Thus, DNA-PK is not required for DNA damage-induced apoptosis, although signaling modulation by FLV infection would cause DNA-PK participation in apoptosis in response to DNA damage. Therefore, our present data would indicate the existence of some unidentified factor(s) amplifying mild DNA damage signals to induce severe cell death. Molecules involved in the DNA-PK-gp70 association or in the overexpression of DNA-PK might be the key to clarifying these mechanisms.

Controlling p53-mediated apoptosis would be one of the most attractive strategies of gene therapy for cancer [46]. The modifier of p53 for strong activation would be crucial to make the *p53*-gene therapy more effective. The mechanism of DNA-PK-associated p53 signaling modification leading to enhanced apoptosis should be clarified not only to understand the complexity of p53 signaling changed by retroviral infection but also to effectively use the p53 function in gene therapy aimed at cancer.

Acknowledgements

This work was supported in part by Research Grants from the National Institute of Radiological Sciences, Chiba, Japan and by a Grant-in-Aid from the Ministry of Education, Culture, Sports, Science and Technology of Japan.

References

[1] Ko LJ, Prives C. p53: puzzle and paradigm. Genes Dev 1996;10:1054–72.

[2] Levine AJ. p53, the cellular gatekeeper for growth and division. Cell 1997;88:323–31.

[3] Vogelstein B, Lane D, Levine AJ. Surfing the p53 network. Nature 2000;408:307–10.

[4] Chehab NH, Malikzay A, Stavridi ES, Harazonetis TD. Phosphorylation of Ser-20 mediates stabilization of human p53 in response to DNA damage. Proc Natl Acad Sci USA 1999;96:13777–82.

[5] Shieh SY, Ikeda M, Taya Y, Prives C. DNA damage-induced phosphorylation of p53 alleviates inhibition by MDM2. Cell 1997;91:325–34.

[6] Barlow C, Brown KD, Deng CX, Tagle DA, Wynshaw-Boris A. ATM selectively regulates distinct p53-dependent cell-cycle checkpoint and apoptotic pathways. Nature Genet 1997;17:453–6.

[7] Woo RA, McLure KG, Lees-Miller SP, Rancourt D, Lee PWK. DNA-dependent protein kinase acts upstream of p53 in response to DNA damage. Nature 1998;394:700–4.

[8] Wang S, Guo M, Ouyang H, Li X, Cordon-Cardo C, Kurimasa A, et al. The catalytic subunit of DNA-dependent protein kinase selectively regulates p53-dependent apoptosis but not cell-cycle arrest. Proc Natl Acad Sci USA 2000;97:1584–8.

[9] Araki R, Fukumura R, Fujimori A, Taya Y, Shiloh Y, Kurimasa A, et al. Enhanced phosphorylation of p53 Serine 18 following DNA damage in DNA-dependent protein kinase catalytic subunit-deficient cells. Cancer Res 1999;59:3543–6.

[10] Banin S, Moyal S, Shieh SY, Taya Y, Anderson CW, Chessa L, et al. Enhanced phosphorylation of p53 by ATM in response to DNA damage. Science 1998;281:1674–7.

[11] Burma S, Kurimasa A, Xie G, Taya Y, Araki R, Abe M, et al. DNA-dependent protein kinase-independent activation of p53 in response to DNA damage. J Biol Chem 1999;274:17139–43.

[12] Cannan CE, Lim DS. The role of ATM in DNA damage responses and cancer. Oncogene 1998;17:3301–8.

[13] Cannan CE, Lim DS, Cimprich KA, Taya Y, Tamai K, Sakaguchi K, et al. Activation of the ATM kinase by ionizing radiation and phosphorylation of p53. Science 1998;281:1677–9.

[14] Jhappan C, Yusufzai TM, Anderson S, Anver MR, Melino G. The p53 response to DNA damage in vivo is independent of DNA-dependent protein kinase. Mol Cell Biol 2000;20:4075–85.

[15] Jimenez GS, Bryntesson F, Torres-Arzayus MI, Priestley A, Beeche M, Saito S, et al. DNA-dependent protein kinase is not required for the p53-dependent response to DNA damage. Nature 1999;400:81–3.

[16] Durocher D, Jackson SP. DNA-PK, ATM and ATR as sensors of DNA damage: variations on a theme? Curr Opin Cell Biol 2001;13:225–31.

[17] Smith GCM, Jackson SP. The DNA-dependent protein kinase. Genes Dev 1999;13:916–34.

[18] Thome M, Schneider P, Hofmann K, Fickenscher H, Meinl E, Neipel F, et al. Viral FLICE-inhibitory proteins (FLIPs) prevent apoptosis induced by death receptors. Nature 1997;386:517–21.

[19] Sevilla L, Aperlo C, Dulic V, Chambard JC, Boutonnet C, Pasquier O, et al. The ets2 transcription factor inhibits apoptosis induced by colony-stimulating factor 1 deprivation of macrophages through a bcl-xL-dependent mechanism. Mol Cell Biol 1999;19:2624–34.

[20] Badley AD, Pilon AA, Landay A, Lynch LH. Mechanisms of HIV-associated lymphocytic apoptosis. Blood 2000;96:2951–64.

[21] Bonzon C, Fan H. Moloney murine leukemia virus-induced preleukemic thymic atrophy and enhanced thymocyte apoptosis correlate with disease pathogenicity. J Virol 1999;73:2434–41.

[22] Hollesberg P. Mechanisms of T-cell activation by human T-cell lymphotropic virus type I. Microbiol Mol Biol Rev 1999;63:308–33.

[23] Kitagawa M, Yamaguchi S, Hasegawa M, Tanaka K, Sado T, Hirokawa K, et al. Friend leukemia virus infection enhances DNA damage-induced apoptosis of hematopoietic cells, causing lethal anemia in C3H hosts. J Virol 2002;76:7790–8.

[24] Kelley LL, Hicks GG, Hsieh FF, Prasher JM, Green WF, Miller MD, et al. Endogenous p53 regulation and function in early stage Friend virus-induced tumor progression differs from that following DNA damage. Oncogene 1998;17:1119–30.

[25] Quang CT, Wessely O, Pironin M, Beug H, Ghysdael J. Cooperation of Spi-1/PU.1 with an activated erythropoietin receptor inhibits apoptosis and Epo-dependent differentiation in primary erythroblasts and induces their Kit ligand-dependent proliferation. EMBO J 1997;16:5639–53.

[26] Pereira R, Quang CT, Lesault I, Dolznig H, Beug H, Ghysdael J. FLI-1 inhibits differentiation and induces proliferation of primary erythroblasts. Oncogene 1999;18:1597–608.

[27] Blunt T, Finnie NJ, Taccioli GE, Smith GCM, Demengeot J, Gottlieb TM, et al. Defective DNA-dependent protein kinase activity is linked to V(D)J recombination and DNA repair defects associated with the murine SCID mutation. Cell 1995;80:813–23.

[28] Kirchgessner CU, Patil CK, Evans JW, Cuomo CA, Fried LM, Carter T, et al. DNA-dependent kinase (p350) as a candidate gene for the murine SCID defect. Science 1995;267:1178–83.

[29] Peterson SR, Kurimasa A, Oshimura M, Dynan WS, Bradbury EM, Chen DJ. Loss of the catalytic subunit of the DNA-dependent protein kinase in DNA double-strand break repair mutant mammalian cells. Proc Natl Acad Sci USA 1995;92:3171–4.

[30] Barlow C, Hirotsune S, Paylor R, Liyanage M, Eckhaus M, Collins F, et al. *ATM*-deficient mice: a paradigm of ataxia telangiectasia. Cell 1996;86:159–71.

[31] Kitagawa M, Matsubara O, Kasuga T. Dynamics of lymphocytic subpopulations in Friend leukemia virus-induced leukemia. Cancer Res 1986;46:3034–9.

[32] Kitagawa M, Kamisaku H, Sado T, Kasuga T. Friend leukemia virus-induced leukemogenesis in fully H-2 incompatible C57BL/6 → C3H radiation bone marrow chimeras. Leukemia 1993;7:1041–6.

[33] Kitagawa M, Aizawa S, Kamisaku H, Hirokawa K, Ikeda H. Protection of retrovirus-induced disease by transplantation of bone marrow cells transduced with MuLV *env* gene via retrovirus vector. Exp Hematol 1999;27:234–41.

[34] Kitagawa M, Takahashi M, Yamaguchi S, Inoue M, Ogawa S, Hirokawa K, et al. Expression of inducible nitric oxide synthase (NOS) in bone marrow cells of myelodysplastic syndromes. Leukemia 1999;13:699–703.

[35] Kitagawa M, Aizawa S, Kamisaku H, Sado T, Ikeda H, Hirokawa K. Distribution of *Fv-4* resistant gene product in Friend leukemia virus-resistant *Fv-4*^{r} mouse strain. Exp Hematol 1996;24:1423–31.

[36] Dignam JD, Martin PL, Shastry BS, Roeder RG. Eukaryotic gene transcription with purified components. Methods Enzymol 1983;101:582–98.

[37] Shangary S, Brown KD, Adamson AW, Edmonson S, Ng B, Pandita TK, et al. Regulation of DNA-dependent protein kinase activity by ionizing radiation-activated Abl kinase is an ATM-dependent process. J Biol Chem 2000;275:30163–8.

[38] Daniel R, Katz RA, Skalka AM. A role for DNA-PK in retroviral DNA integration. Science 1999;284:644–7.

[39] Lees-Miller SP, Sakaguchi K, Ullrich SJ, Appella E, Anderson CW. Human DNA-activated protein kinase phosphorylates serines 15 and 37 in the amino-terminal transactivation domain of human p53. Mol Cell Biol 1992;12:5041–9.

[40] Ikeda H, Odaka T. Cellular expression of murine leukemia virus gp-70-related antigen on thymocytes of uninfected mice correlated with *Fv-4* gene-controlled resistance to Friend leukemia virus infection. Virology 1983;128:127–39.

[41] Howard J, Ung Y, Adachi D, Ben-David Y. p53-independent tumor growth and in vitro cell survival for F-MuLV-induced erythroleukemias. Cell Growth Differ 1996;7:1651–60.

[42] Jeggo PA. DNA-PK: at the cross-roads of biochemistry and genetics. Mutat Res 1997;384:1–14.

[43] Gurley KE, Kemp CJ. Synthetic lethality between mutation in ATM and DNA-PK$_{CS}$ during murine embryogenesis. Curr Biol 2001;11:191–4.
[44] Daniel R, Katz RA, Merkel G, Hittle JC, Yen TJ, Skalka AM. Wortmanin potentiates integrase-mediated killing of lymphocytes and reduces the efficiency of stable transduction by retroviruses. Mol Cell Biol 2001;21:1164–72.
[45] Woo RA, Jack MT, Xu Y, Burma S, Chen DJ, Lee PWK. DNA damage-induced apoptosis requires the DNA-dependent protein kinase, and is mediated by the latent population of p53. EMBO J 2002;21:3000–8.
[46] McCormick F. Cancer gene therapy: fringe or cutting edge? Nat Rev Cancer 2001;1:130–41.

Available online at www.sciencedirect.com
SCIENCE DIRECT®
Leukemia Research 28 (2004) 487–494
Leukemia Research
www.elsevier.com/locate/leukres

Differential expression of survivin in bone marrow cells from patients with acute lymphocytic leukemia and chronic lymphocytic leukemia

Yasunori Nakagawa [a,b,1], Shuichi Yamaguchi [a,1], Maki Hasegawa [a], Tetsuo Nemoto [c], Miori Inoue [a], Kenshi Suzuki [b], Katsuiku Hirokawa [a], Masanobu Kitagawa [a,*]

[a] *Department of Pathology and Immunology, Aging and Developmental Sciences, Graduate School, Tokyo Medical and Dental University, 1-5-45 Yushima, Bunkyo-ku, Tokyo 113-8519, Japan*
[b] *Department of Hematology, Japanese Red Cross Medical Center, Tokyo, Japan*
[c] *Department of Pathology, Tokyo Medical and Dental University, Tokyo, Japan*

Received 29 July 2003; accepted 3 October 2003

Abstract

Survivin, a member of the inhibitor of apoptosis protein (IAP) gene family, has been detected widely in fetal tissue and in a variety of human malignancies. In the current study, we investigated the expression of IAP family proteins in bone marrow samples from acute lymphocytic leukemia (ALL), chronic lymphocytic leukemia (CLL) and control cases by quantitative real-time RT-PCR method and an immunohistochemical approach. Overexpression of survivin and cIAP2 mRNA was significant in CLL bone marrow cells ($P < 0.05$, respectively) compared with control samples. By immunohistochemistry, survivin was detected in a few scattered myeloid cells in all cases of control bone marrow. Concerning the ALL bone marrow, more than half the cases demonstrated positive expression of survivin (8 out of 13), while the majority of CLL cases (20 out of 21) exhibited intense expression of survivin. The differential subcellular localization of survivin was distinct between ALL and CLL cases. ALL cells essentially revealed nuclear localization of survivin as well as cytoplasmic signals in some cases, while CLL cells from the majority of cases predominantly showed cytoplasmic expression. Next, RT-PCR was performed for the expression of survivin and its splicing variant, survivin-2B and survivin-ΔEx3 in ALL and CLL cells, as the distribution of these variants would be regulated by nuclear/cytoplasmic transport system. In both ALL and CLL bone marrow samples, the expression of wild-type survivin was more predominant than that of survivin-2B or survivin-ΔEx3, although the expression of survivin-ΔEx3 was prominent in samples from survivin-expressing ALL cases. Thus, the splicing of survivin mRNA may be differently regulated in ALL and CLL cells, causing distinct manners of nuclear/cytoplasmic transport of survivin protein. In conclusion, our observations indicate a differential regulatory mechanism for the expression of IAP family proteins in ALL and CLL cells, although the functions of IAP families and the mechanisms of nuclear/cytoplasmic transport of survivin should be clarified in future studies.

Keywords: Survivin; IAP; Bone marrow; ALL; CLL

1. Introduction

The regulation of apoptotic cell death may have a profound effect on the pathogenesis and progression of hematological malignancies. Chronic lymphocytic leukemia (CLL) is characterized by clonal expansion of relatively mature B cells with a high percentage of cells arrested in the non-proliferative G0/G1 cell cycle phase [1,2]. The progressive rise of lymphocytes, despite the very low proportion of proliferating cells, has led to the notion that the pathogenesis of CLL is primarily related to defective apoptosis. In contrast, acute lymphocytic leukemia (ALL) cells exhibit highly proliferative character with a very low percentage of apoptotic cells [1,3,4]. Thus, ALL and CLL cells may be regulated by different types of cell-proliferation/cell-death signaling pathway. To begin to clarify the antiapoptotic pathways in lymphocytic leukemias, the expression and modulation of the family of inhibitor of apoptosis proteins (IAPs), especially survivin, were investigated and compared in control, ALL and CLL bone marrow samples.

Survivin is expressed widely in fetal tissues, but becomes restricted during development, and appears to be negligibly expressed in the majority of terminally differentiated adult tissues [5,6]. However, analysis of the differences in gene expression between normal and tumor cells has revealed that survivin is one of the genes most consistently overexpressed

* Corresponding author. Tel.: +81-3-5803-5399; fax: +81-3-5803-0123.
E-mail address: masa.pth2@med.tmd.ac.jp (M. Kitagawa).
[1] These authors contributed equally to this work.

0145-2126/$ – see front matter © 2003 Elsevier Ltd. All rights reserved.
doi:10.1016/j.leukres.2003.10.013

in tumor cells relative to normal tissue [7]. In fact, survivin is prominently expressed in transformed cell lines and in many of the human cancers including hematopoietic cell tumors [8].

As with other IAP family proteins, survivin blocks apoptosis induced by a variety of apoptotic triggers [9,10]. Although the exact biochemical mechanism by which survivin suppresses apoptosis has been debated, survivin is known to bind directly to and inhibit caspase-3 and -7, which act as terminal effectors in apoptotic protease cascades [10,11]. Survivin is usually detected in the cytoplasm of tumor cells, and is therefore widely regarded as a cytoplasmic protein [5,12,13]. However, several studies have shown nuclear accumulation of survivin in gastric cancer cells [14] and lung cancer cells [15]. Thus, the mechanisms that control its nuclear-cytoplasmic localizations in tumor cells are still controversial.

Many cellular proteins either reside in the nucleus or shuttle between the nucleus and the cytoplasm across the nuclear envelope. In a recent study, survivin was shown to be a nuclear shuttling protein that was actively exported from the nucleus via the chromosome region maintenance 1 (CRM1)-dependent pathway [15]. CRM1 was shown to be a receptor for the nuclear export signal that bound to the nuclear export sequences of the proteins. Thus, the molecular export sequences are very important in determining the subcellular localization of proteins. Differences in the amino acid sequence of the carboxy-terminal domain of survivin determine the dramatically different localization of survivin and its splice variant, survivin-ΔEx3. Survivin-ΔEx3 lacks exon 3 but has additional sequences that could mediate its strong nuclear accumulation. Therefore, wild-type survivin localizes to the cytoplasm, while survivin-ΔEx3 accumulates in the nucleus.

Here, in the present study, overall survivin expression was significantly up-regulated in the bone marrow cells from ALL and CLL compared with the control bone marrow. However, different localization of survivin was shown by the nuclear expression in ALL and the cytoplasmic expression in CLL. Expression of other IAPs including NAIP, cIAP1, cIAP2 and XIAP, all of which appeared to suppress apoptosis by caspase and procaspase inhibition [16–19] was also determined in these samples and the significance of IAP family protein expression in lymphocytic leukemias was discussed.

2. Materials and methods

2.1. Patients

Formalin-fixed paraffin-embedded bone marrow aspiration samples from 13 patients with adult-onset ALL (7 with B-ALL and 6 with T-ALL; male:female = 5:8; age: median 48, maximum 78, minimum 19), 21 patients with B-CLL (male:female = 11:10; age: median 57, maximum 87, minimum 49) and 13 cases with no hematological disorders as age-matched normal controls (male:female = 13:0; age: median 63, maximum 76, minimum 51) were analyzed. To rule out the influence of aging effect on bone marrow cells, ALL cases with adult-onset were analyzed and cases with childhood ALL were excluded from the study. Diagnosis was based on standard clinical and laboratory criteria, including cell morphology [20–22]. All samples were collected at the time of the initial aspiration biopsy and the samples from ALL and CLL exhibited proliferation of the blastic cells accounting for more than 80% of the total bone marrow cells. The patients were not infected with specific viruses including HTLV-1 and had not been treated with therapeutic drugs prior to the study. The procedures followed were in accord with the ethical standards established by the ethics committee of Tokyo Medical and Dental University.

2.2. Identification of apoptotic cells

To determine apoptotic cells, the terminal deoxy-transferase (TdT)-mediated dUTP nick-end labeling (TUNEL) method was used for the assay as described previously [23]. Briefly, tissue sections were deparaffinized and incubated with proteinase K (prediluted, DAKO, Glostrup, Denmark) for 15 m at room temperature. After washing, TdT, fluorescein isothiocyanate (FITC)-dUTP and dATP (Boehringer Mannheim, Mannheim, Germany) were applied to the sections, which were then incubated in a moist chamber for 60 min at 37 °C. Anti-FITC-conjugated antibody-peroxidase (POD converter, Boehringer Mannheim) was employed for detecting FITC-dUTP labeling, followed by color development with DAB containing 0.3% hydrogen peroxide solution. Sections were then observed under microscopy and the TUNEL-positive cell ratio was determined by dividing the cell number of positively stained cells by the total cell number (counting more than 1,000 cells).

2.3. RNA preparation and quantitative assay for IAP family proteins using TaqMan RT-PCR

The RNA was extracted from the frozen bone marrow samples from seven cases with ALL (four with B-ALL and three with T-ALL), seven cases with B-CLL and eight cases with no hematological disorders using an RNeasy Mini Kit (Qiagen, Valencia, CA) according to the manufacturer's directions. For quantitative RT-PCR, fluorescent hybridization probes, TaqMan PCR Core Reagents Kit with AmpliTaq Gold (Perkin-Elmer Cetus, Norwalk, CT) were used with the ABI Prism 7900HT Sequence Detection System (Perkin-Elmer, Foster City, CA). Oligonucleotides as specific primers and TaqMan probes for IAP family and glutaraldehyde-3-phosphate dehydrogenase (GAPDH) mRNA were synthesized by a commercial laboratory (Perkin-Elmer Cetus). The primers and TaqMan probes were as follows. Sequences of the forward primer for survivin

mRNA were 5′-TGCCTGGCAGCCCTTTC-3′ and the reverse primer, 5′-CCTCCAAGAAGGGCCAGTTC-3′; the sequence of the TaqMan probe was 5′-CAAGGACCACCGCATCTCTACATTC-3′. For cIAP1 mRNA, sequences of the forward primer were 5′-CAGCCTGAGCAGCTTGCAA-3′ and the reverse primer, 5′-CAAGCCACCATCACAACAAAA-3′; the TaqMan probe was 5′-TTTATTATGTGGGTCGCAATGATGATGTCAAA-3′. For cIAP2 mRNA, sequences of the forward primer were 5′-TCCGTCAAGTTCAAGCCAGTT-3′ and the reverse primer, 5′-TCTCCTGGGCTGTCTGATGTG-3′; the sequence of the TaqMan probe was 5′-CCCTCATCTACTTGAACAGCTGCTAT-3′. Sequences of the forward primer for NAIP mRNA were 5′-GCTTCACAGCGCATCGAA-3′ and the reverse primer, 5′-GCTGGGCGGATGCTTTC-3′; the sequence of the TaqMan probe was 5′-CCATTTAAACCACAGCAGAGGCTTTAT-3′. Sequences of the forward primer for XIAP mRNA were 5′-AGTGGTAGTCCTGTTTCAGCATCA-3′ and the reverse primer, 5′-CCGCACGGTATCTCCTTCA-3′; the sequence of the TaqMan probe was 5′-CACTGGCACGAGCAGGGTTTCTTTATACTG-3′. Sequence of the forward primer for GAPDH mRNA were 5′-GAAGGTGAAGGTCGGAGT-3′ and the reverse primer, 5′-GAAGATGGTGATGGGATTTC-3′; the sequence of the TaqMan probe was 5′-CAAGCTTCCCGTTCTCAGCC-3′. Conditions of one-step RT-PCR were as follows: 30 min at 48 °C (stage 1, reverse transcription), 10 min at 95 °C (stage 2, RT inactivation and AmpliTaq Gold activation) and then 40 cycles of amplification for 15 s at 95 °C and 1 min at 60 °C (stage 3, PCR). Expression of survivin and other IAP family proteins was quantitated according to the method described elsewhere [24]. Briefly, the intensity of reaction was evaluated by the quantity of total RNA of Raji cells (ng) corresponding to the initial PCR cycle numbers to reveal the linear increase of reaction intensity (threshold cycle) in each sample on the logarithmic scale standard curve. Data of the Raji RNA quantity (ng) for IAP family were normalized by the data for GAPDH in each sample.

2.4. Immunohistochemistry for survivin, p53 and cell markers

Four micrometer-thick tissue sections of bone marrow from control, ALL and CLL cases were cut on slides covered with adhesive. Sections were deparaffinized, and endogenous peroxidase was quenched with 1.5% hydrogen peroxide in methanol for 10 min. Antibodies were applied to identify survivin, to characterize B cells (CD20) and T cells (CD45RO), and to identify accumulation of p53 protein. Primary antibodies included polyclonal rabbit antibody against human survivin (SURV 11-A, Alpha Diagnostic International, San Antonio, TX), monoclonal antibodies against CD20 (DAKO), CD45RO (DAKO) and p53 (Novocastra Laboratories Ltd., Newcastle, UK). All sections were developed using biotin-conjugated secondary antibodies against rabbit IgG or mouse IgG followed by a sensitive peroxidase-conjugated streptavidin system (DAKO) with DAB as the chromogen. Negative control staining procedure was performed using rabbit or mouse immunoglobulin of irrelevant specificity substituted with the primary antibody in each staining.

Phenotype determination of survivin-expressing cells was performed by double immunostaining using polyclonal antibody against survivin and monoclonal antibody against CD20 or CD45RO followed by the peroxidase–DAB development system and then, alkaline phosphatase-conjugated anti-mouse IgG (DAKO) followed by development with the alkaline phosphatase-nitroblue tetrazolium chloride-5-bromo-4-chloro-3-indolyl phosphatase development system (DAKO).

2.5. RT-PCR analysis for survivin and splice variants, survivin-2B and survivin-ΔEx3

To determine the pattern for the splicing of survivin, RT-PCR analysis was performed using specific primers that could distinguish each type of splicing variant, survivn-2B and survivin-ΔEx3, by product size [25]. The PCR reaction was performed as described elsewhere [26,27]. Briefly, 100 ng of the RNA was used for RT-PCR. For complementary (c)DNA synthesis, 100 ng in 4 μl of sample RNA solution was heated at 65 °C for 5 min and cooled rapidly. After adding 20 U of ribonuclease inhibitor (Takara, Japan), 1 μl of 1.25 mM dNTP (dATP, dCTP, dGTP, dTTP, Pharmacia, Uppsala, Sweden) and 20 U of Rous-associated virus reverse transcriptase (Takara Biomedicals, Kyoto, Japan), the mixture was incubated at 40 °C for 30 min, then heated at 94 °C for 5 min and cooled rapidly. Oligonucleotides as specific primers for survivin were synthesized by a commercial laboratory (Invitrogen Life Technologies, Tokyo, Japan). The sequences of primers were as follows: forward primer, 5′-ACCGCATCTCTACATTCAAG-3′ and the reverse 5′-CTTTCTTCGCAGTTTCCTC-3′. In the control reaction β-actin was also determined using the forward primer 5′-AAGAGAGGCATCCTCACCCT-3′, and the reverse 5′-TACATGGCTGGGGTGTTGAA-3′. The PCR reaction mixture contained 10 μl of cDNA, 10 μl of 10 × PCR buffer, 11 μl of 20 mM $MgCl_2$, 16 μl of 1.25 M dNTP, 42.5 μl of DEPC-water, 100 pM forward and reverse primers, and 2.5 U of thermostable Taq polymerase (Perkin-Elmer Cetus, Norwalk, CT, USA). The amplification was achieved with a DNA thermal cycler (Perkin-Elmer Cetus). After denaturing at 94 °C for 10 min, the amplification was conducted for 45 cycles at 94 °C for 30 s, 55 °C for 30 s and 72 °C for 60 s. This was followed by re-extension for 10 min at 72 °C. Ten microliters aliquots of the product samples were analyzed by electrophoresis on a 1.8% agarose gel and visualized by UV fluorescence after staining with ethidium bromide. The expected sizes of the PCR product were 342 bp for wild-type survivin, 411 bp for survivin-2B, 224 bp for survivin-ΔEx3 and 218 bp for β-actin. φX174/Hae III-cut DNA was run in parallel as a molecular size marker.

2.6. Statistical analysis

Statistically significant differences were determined using the Mann–Whitney's *U*-test.

3. Results

3.1. Apoptotic cell ratio of the bone marrow cells from ALL, CLL, and control cases

To identify the apoptotic cells in the bone marrow samples, the TUNEL method was performed on paraffin-embedded sections. We compared the overall TUNEL-positive cell ratio of control bone marrow with the ratio of ALL or CLL samples, although the apoptotic cells of control bone marrow were not necessarily the lymphoid cells. The apoptotic cell ratio was rather low even in the control bone marrow samples as shown in Table 1, however, the ratio was lower in ALL and CLL cases than in control cases. Differences were significant between ALL and control ($P < 0.01$ by the Mann–Whitney's *U*-test) and CLL and control cases ($P < 0.0001$). ALL cells exhibited relatively lower frequency of TUNEL-positive signals than CLL cells ($P < 0.0001$). These findings suggested that apoptosis was actually infrequent in ALL cells as well as in CLL cells.

3.2. Expression of mRNA for IAP family proteins determined by real-time quantitative PCR

To quantitate the mRNA expression levels of IAP family proteins in lymphocytic leukemia cells, real-time quantitative RT-PCR was performed using bone marrow samples from ALL, CLL and control cases. The expression of mRNA for survivin, cIAP1, cIAP2, NAIP and XIAP was found in all of the control samples although the expression levels varied. Thus, the expression intensity of IAP family proteins was demonstrated as the percentage of control in each group. Differences were significant between survivin expression of CLL and control ($P < 0.05$) and cIAP2 expression of CLL and control ($P < 0.05$) (Fig. 1). The intensities of mRNA expression of cIAP1, cIAP2, NAIP and XIAP proteins in ALL cases tended to be higher than the intensity of control cases, although the differences were not significant. This is caused by the fact that some of the ALL cases revealed very high expression, while other ALL cases had as low expression as control cases. No significant differences were found between survivin expression and patients' age, sex or phenotypic character of leukemic cells (B cell-lineage or T cell-lineage). These results indicated that the expression of survivin and cIAP2 would be significant in CLL bone marrow, whereas survivin as well as other IAP family proteins might possibly have a role only in some ALL cases.

Table 1
Apoptotic cell ratio of the bone marrow from ALL, CLL and control cases

Cases	TUNEL-positive cell ratio (%)[a]	
	Median	Maximum–minimum
ALL	0.044	0.38–0.0032[b,c]
CLL	0.13	0.98–0.011[c,d]
Control	1.08	3.65–0.58[b,d]

[a] Values indicate the median value, the maximum and the minimum values.

[b] Differences were significant between the TUNEL-positive cell ratio of ALL and control cases ($P < 0.01$) by the Mann–Whitney's *U*-test.

[c] Differences were significant between the TUNEL-positive cell ratio of ALL and CLL cases ($P < 0.0001$) by the Mann–Whitney's *U*-test.

[d] Differences were significant between the TUNEL-positive cell ratio of CLL and control cases ($P < 0.0001$) by the Mann–Whitney's *U*-test.

3.3. Immunohistochemical localization of survivin in the bone marrow of control, ALL and CLL cases

To investigate the localization of survivin, immunohistochemical staining was performed in bone marrow samples from ALL, CLL and control cases. ALL cells exhibited various degrees of survivin expression from case to case. In one case, the majority of cells stained positively, while in seven cases, staining was partial (Table 2). In five cases of ALL, survivin was not detected immunohistochemically. At the cellular level, survivin signals in ALL cells were predominantly localized to the nucleus (Fig. 2A and B), although in some cases, prominent reaction was also observed in the cytoplasm of ALL cases. Moreover, survivin was detected in most of the bone marrow samples from CLL cases by immunohistochemical staining (20 out of 21 cases). Positive staining was observed in the majority of CLL cells in half the cases (10 out of 20 survivin-positive cases), while other cases exhibited positive signals in some CLL cells (Table 2). In contrast to the subcellular localization of survivin in ALL cases, survivin in CLL cells was predominantly localized to the cytoplasm with minimal nuclear staining (Fig. 2C and D). By contrast, survivin was detected in only a few scattered myeloid cells of the control bone marrow samples (Fig. 2E). The subcellular localization was mainly cytoplasmic but partly nuclear. The staining pattern and intensity of the control bone marrow was constant between different samples. Tissue sections that were reacted with preimmune rabbit antibody with irrelevant specificity showed no significant staining in all of the samples (not shown). Double staining procedure revealed survivin-expressing cells were CD20-positive cells both in B-ALL and B-CLL (Fig. 3A and B) suggesting that these cells were actually leukemic cells.

3.4. Expression of survivin and splice variants, survivin-2B and survivin-ΔEx3 in ALL, CLL and control cases

To examine whether the differential subcellular localization of survivin between ALL and CLL cases was due to the difference in nuclear/cytoplasmic transport state, RT-PCR analysis was performed to distinguish the wild-type and

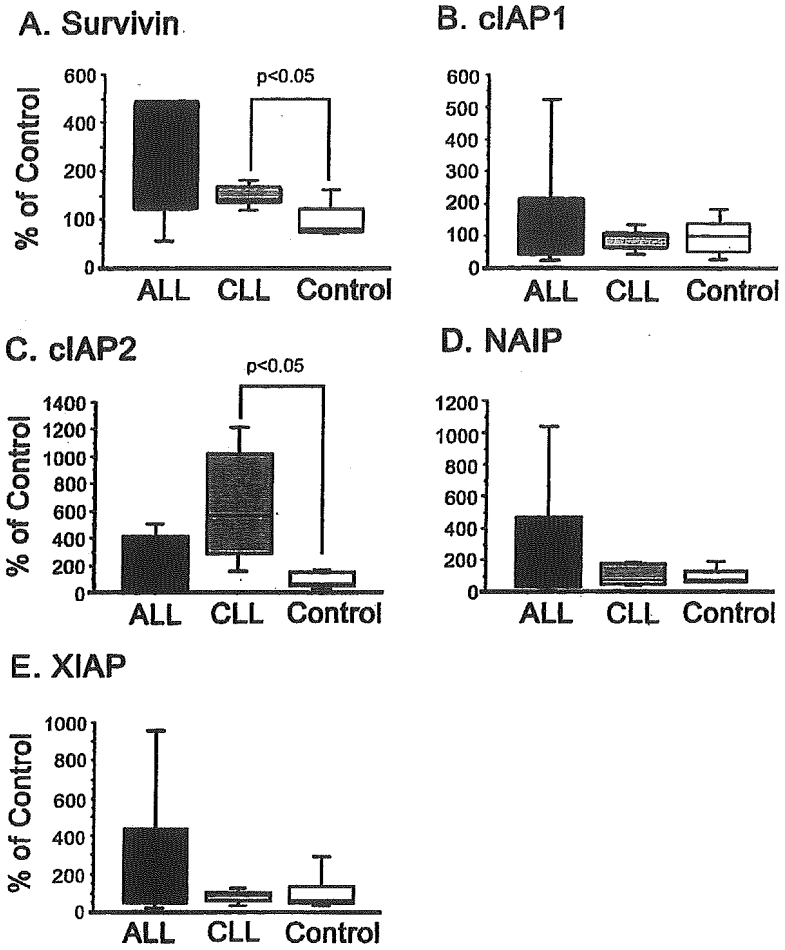

Fig. 1. ((A)–(E)) Quantitative RT-PCR analysis for IAP family proteins, survivin, cIAP1, cIAP2, NAIP and XIAP. Relative intensity was calculated as intensity of reaction of IAP family (total Raji RNA (ng))/intensity of reaction of GAPDH (total Raji RNA (ng)). The intensity of expression from ALL and CLL samples is indicated as the percentage of the intensity of control samples. The box plot graphs indicate the value of ALL, CLL and control cases. Bars indicate 90% tile and 10% tile and box indicates 75% tile to 25% tile. Differences were significant between survivin expression in CLL and control cases ($P < 0.05$) and cIAP2 expression in CLL and control cases ($P < 0.05$) by the Mann–Whitney's U-test.

splice variants of survivin. In an in vitro transfection study, the wild-type survivin and the splice variant survivin-2B have been shown to localize to the cytoplasm. In contrast, another variant, survivin-ΔEx3, has a carboxy-terminal end that is different from other types of survivin and mediates strong nuclear accumulation [15]. Thus, the difference in the splicing patterns of survivin would indicate the difference in the state of nuclear/cytoplasmic transport system. In ALL and CLL bone marrow samples, predominant expression was confined to the wild-type survivin, although a weak expression of survivin-2B and survivin-ΔEx3 was also identified (Fig. 4). The splicing for survivin-ΔEx3, appeared more frequent in ALL cases compared with CLL cases, although the expression of wild-type survivin was the strongest even in ALL cases. Therefore, splicing patterns seemed different between ALL and CLL cells. These findings suggested that

Table 2
Immunohistochemical localization of survivin in the bone marrow from ALL, CLL and control cases

Cases	Number of cases					Positive cases (%)	Subcellular localization
	Total	+++	++	+	−		
ALL	13	1	4	3	5	62	Nuclear > cytoplasmic
CLL	21	10	5	5	1	95	Cytoplasmic
Control	13	0	0	0	13	0	Nuclear/cytoplasmic, scattered myeloid cells

+++: the majority of cells exhibited intense expression; ++: more than 50% of cells revealed positive signal; +: positive staining was observed in 10–50% of cells; −: positive cells were less than 10%.

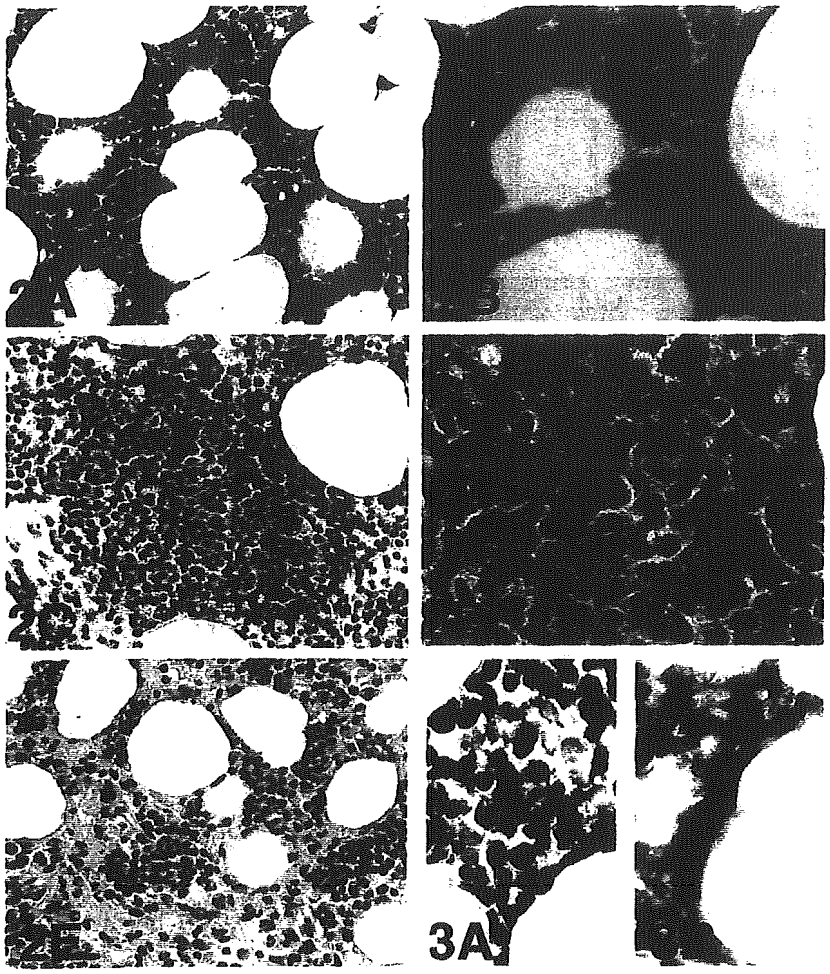

Figs. 2–3. (2) Immunohistochemical localization of survivin in the bone marrow from ALL ((A) and (B)), CLL ((C) and (D)) and control (E) cases. Development procedures were performed using the peroxidase–DAB system (brown). Note that the majority of cells were positively stained in ALL and CLL cases, while only a few myeloid cells exhibited positive signals in control bone marrow ((A), (C) and (E), original magnification 200×). ALL cells showed striking signals in the nucleus as well as in the cytoplasm, whereas positive signals in CLL cells were mainly cytoplasmic and not nuclear ((B) and (D), original magnification 400×). (3) Double immunostaining for survivin and CD20 in the bone marrow from B-ALL (A) and B-CLL cases (B) (original magnification 200×). For double immunostaining, development procedures were performed using the peroxidase–DAB system for survivin (brown) and the alkaline phosphatase-nitroblue tetrazolium system for CD20 (blue). In both ALL (A) and CLL (B) cases, survivin-positive cells (brown) were also positive for CD20 antigen (blue) suggesting that the leukemic cell expressed survivin.

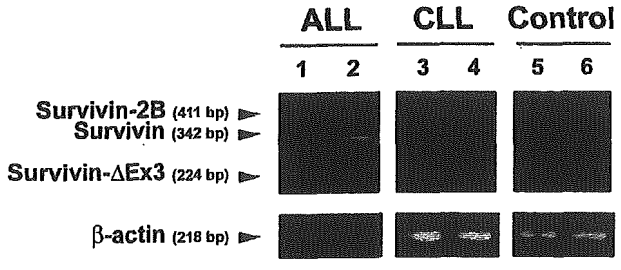

Fig. 4. RT-PCR analysis for the expression of wild-type survivin and the splice variant survivin-2B and survivin-ΔEx3 in ALL (lanes 1 and 2), CLL (lanes 3 and 4) and control bone marrow (lanes 5 and 6). In ALL and CLL samples, the predominant expression was observed in the 342 bp wild-type survivin. However, note that ALL cases have distinct 224 bp signals for survivin-ΔEx3, while CLL cases exhibit very weak 411 bp survivin-2B signals other than wild-type survivin. In some ALL cases, the expression of survivin-ΔEx3 was prominent as shown in lane 2.

the mechanism of the nuclear/cytoplasmic transport system of survivin such as the CRM1 system or the distribution of survivin-binding proteins such as caspases might be differently regulated in ALL cells compared with CLL cells.

3.5. p53 expression in the bone marrow cells of ALL and CLL cases

To determine whether p53-dependent apoptotic pathways were associated with the expression of survivin in ALL and CLL cases, immunohistochemical staining was performed for detecting p53 accumulation in bone marrow samples. As expected from the previous studies [2,4], accumulation of p53 protein was not frequent in ALL and CLL cells in the present study. A positive reaction was observed only in 8% of ALL (1 out of 13 cases) and 10% of CLL cases (2 out of 21 cases). Because the overexpression of survivin was

observed in more than half the ALL cases and the majority of CLL cases, these results suggested that survivin expression in ALL and CLL cases would not be associated with p53 mutation.

4. Discussion

Regarding the survivin expression in lymphocytic leukemia cells, previous studies have revealed an overexpression in some ALL cases [28,29] including adult T-cell leukemia [30] or a significant expression in B-CLL cases [31], while other group indicated that survivin was undetectable in the majority of B-CLL samples [32]. The in vitro data on mononuclear cells from the peripheral blood or bone marrow demonstrated that B-CLL cells expressed survivin on CD40 stimulation and that survivin was the only IAP whose expression was induced by the CD40 ligand (CD40L) [31]. CD40 belongs to the tumor necrosis factor (TNF) receptor superfamily [33] and its stimulation appears to rescue B-CLL cells from apoptosis and induce proliferation [34]. In CLL patients, CD40L would be provided as microenvironmental stimuli by activated $CD4^+$ T cells in the bone marrow. The present data indicated that not only survivin but also cIAP2 exhibited significant overexpression in the bone marrow from CLL patients in vivo. Thus, in CLL bone marrow, multiple microenvironmental factors other than the CD40–CD40L system may also influence the expression of IAP family proteins.

In ALL samples, IAP family expression patterns other than survivin were not uniform in the present study. Some cases exhibited very strong expression, while others revealed an almost normal level of expression. As a result, although the mean intensities of cIAP1, NAIP and XIAP in ALL were higher than those of control cases, the differences were not significant between ALL and control groups. Thus, several IAP family proteins other than survivin might also play a role in some ALL cases but may not be the general factors that regulate apoptotic pathways in ALL cells.

Immunohistochemical staining revealed a very high frequency of survivin expression in CLL cells and relatively high frequency in ALL cells in the present study. Thus, immunohistochemical analysis would be useful for detecting the few remaining leukemic cells after treatment and the very early stage of leukemic relapse of ALL/CLL cases on formalin-fixed routine bone marrow aspiration samples. We confirmed that the condition in leukemic relapse did not alter the state of survivin expression in several samples from ALL and CLL cases, however, further study should be made to clarify the influence of chemotherapeutic agents on the expression patterns of survivin.

Two splice variants of survivin, survivin-ΔEx3 and survivin-2B, have been identified [25]. Study on the regulation of alternative splicing is still a new and intriguing area. Thus, how different splice forms are turned on and off is still controversial except for several instances [35]. Genetic events in ALL/CLL pathogenesis might involve and alter the splicing mechanism of survivin, although a future study should clarify the details. By transfection experiments, survivin-ΔEx3 conserves antiapoptotic properties, while survivin-2B has a markedly reduced antiapoptotic potential. In the present study, ALL cases and CLL cases exhibited enhanced expression of wild-type survivin as well as survivin-2B, while survivin-ΔEx3 was more intensely expressed in ALL cases than in CLL cases. These variants of survivin might contribute to the suppression of the apoptotic process in the bone marrow cells as expected from the present TUNEL data.

It is difficult to explain the difference in apoptotic character of ALL and CLL only by the expression of survivin and cIAP2 at this moment. However, it is possible that the ability of survivin to counteract apoptosis is modulated by its localization to the nucleus or the cytoplasm of the cell [15]. In addition to its anti-apoptotic function, survivin also plays a role in the regulation of cell cycle progression during mitosis [8]. Highly proliferative activity of ALL cells but low proliferative activity of CLL cells might be associated with the differential expression pattern of survivin.

Wild-type p53, but not mutant p53, represses survivin expression at both the mRNA and protein levels [36]. The modification of chromatin within the survivin promoter would be a molecular explanation for the silencing of survivin gene transcription by p53 [37]. On the other hand, the over-expression of exogenous survivin protein rescues cells from p53-induced apoptosis in a dose-dependent manner, suggesting that loss of survivin mediates in part the p53-dependent apoptotic pathway [37]. In contrast to the high frequency of p53 mutations in many of the solid cancers, ALL (5–17%) and CLL (10–20%) cases have been shown to demonstrate a rather low frequency of p53 mutation [2,4]. We also observed that immunohistochemical accumulation of p53 was present only in 8% of cases with ALL and 10% of CLL cases. Therefore, p53 mutation would not appear to be the major factor controlling the overexpression of survivin in the bone marrow of ALL and CLL cases.

Acknowledgements

This work was supported in part by a grant-in-aid from the Ministry of Education, Culture, Sports, Science and Technology of Japan (No.14570180).

References

[1] Andreeff M, Darzynkiewicz Z, Sharpless TK, Clarkson BD, Melamed MR. Discrimination of human leukemia subtypes by flow cytometric analysis of cellular DNA and RNA. Blood 1980;55:282–3.
[2] Meinhardt G, Wendtner C-M, Hallek M. Molecular pathogenesis of chronic lymphocytic leukemia: factors and signaling pathways regulating cell growth and survival. J Mol Med 1999;77:282–93.

[3] Ball LM, Pope J, Howard CV, Eccles P, van Velzen D. PCNA Ki-67 dissociation in childhood acute lymphoblastic leukaemia. An immunofluorescent laser confocal scanning microscopical study. Cell Biol Int 1994;18:869–74.
[4] Krug U, Ganser A, Koeffler HP. Tumor suppressor genes in normal and malignant hematopoiesis. Oncogene 2002;21:3475–95.
[5] Ambrosini G, Adida C, Altieri DC. A novel anti-apoptosis gene, *survivin*, expressed in cancer and lymphoma. Nat Med 1997;3:917–21.
[6] Adida C, Crotty PL, McGrath J, Berrebi D, Diebold J, Altieri DC. Developmentally regulated expression of the novel cancer anti-apoptotic gene survivin in human and mouse differentiation. Am J Pathol 1998;152:43–9.
[7] Velculescu VE, Madden S, Zhang L, Lash AE, Yu J, Rago C, et al. Analysis of human transcriptomes. Nat Genet 1999;23:387–8.
[8] Altieri DC, Marchisio C. Survivin apoptosis: an interloper between cell death and cell proliferation in cancer. Lab Invest 1999;79:1327–33.
[9] LaCasse EC, Baird S, Korneluk RG, MacKenzie AE. The inhibitors of apoptosis (IAPs) and their emerging role in cancer. Oncogene 1998;17:3247–59.
[10] Tamm I, Wang Y, Sausville E, Scudiero DA, Vigna N, Oltersdorf T, et al. IAP-family protein survivin inhibits caspase activity and apoptosis induced by Fas (CD95), Bax, caspases, and anticancer drugs. Cancer Res 1998;58:5315–20.
[11] Shin S, Sung B-J, Cho Y-S, Kim H-J, Ha N-C, Hwang J-I, et al. An anti-apoptotic protein human survivin is a direct inhibitor of caspase-3 and -7. Biochemistry 2001;40:1117–23.
[12] Gianani R, Jarboe E, Orlicky D, Frost M, Bobak J, Lehner R. Expression of survivin in normal, hyperplastic, and neoplastic colonic mucosa. Hum Pathol 2001;32:119–25.
[13] Kawasaki H, Toyoda M, Shinohara H, Okuda J, Watanabe I, Yamamoto T, et al. Expression of survivin correlates with apoptosis, proliferation, and angiogenesis during human colorectal tumorigenesis. Cancer 2001;91:2026–32.
[14] Okada E, Murai Y, Matsui K, Ishizawa S, Cheng C, Masuda M, et al. Survivin expression in tumor cell nuclei is predictive of a favorable prognosis in gastric cancer patients. Cancer Lett 2001;163:109–16.
[15] Rodriguez JA, Span SW, Ferreira CGM, Kruyt FAE, Giaccone G. CRM1-mediated nuclear export determines the cytoplasmic localization of the antiapoptotic protein survivin. Exp Cell Res 2002;275:44–53.
[16] Rothe M, Pan MG, Henzei WJ, Ayres TM, Goeddel DV. The TNFR2–TRAF signaling complex contains two novel proteins related to baculoviral inhibitor of apoptosis proteins. Cell 1995;83:1243–52.
[17] Duckett CS, Nava VE, Gedrich RW, Clem RJ, Van Dongen JL, Gilfillan MC, et al. A conserved family of cellular genes related to the baculovirus IAP gene and encoding apoptosis inhibitors. EMBO J 1996;15:2685–94.
[18] Liston P, Roy N, Tamai K, Lefebvre C, Baird S, Cherton-Horvat G, et al. Suppression of apoptosis in mammalian cells by NAIP and a related family of IAP genes. Nature 1996;379:349–53.
[19] Roy N, Dereraux QL, Takahashi R, Salvesen GS, Reed JC. The cIAP-1 and cIAP-2 proteins are distinct inhibitors of specific caspases. EMBO J 1997;16:6914–25.
[20] Harris NL, Jaffe ES, Stein H, Banks PM, Chan JK, Cleary ML, et al. A revised European-American classification of lymphoid neoplasms: a proposal from the International Lymphoma Study Group. Blood 1994;84:1361–92.
[21] Harris NL, Jaffe ES, Diebold J, Flandrin G, Muller-Hermelink K, Vardiman J, et al. World Health Organization classification of neoplastic diseases of the hematopoietic and lymphoid tissues: report of the Clinical Advisory Committee Meeting—Airlie House, Virginia, November 1997. J Clin Oncol 1999;17:3835–49.
[22] Matutes E, Owusu-Ankomah K, Morilla R, Garcia Marco J, Houlihau A, Que TH, et al. The immunological profile of B-cell disorders and proposal of a scoring system for the diagnosis of CLL. Leukemia 1994;8:1640–5.
[23] Kitagawa M, Yamaguchi S, Takahashi M, Tanizawa T, Hirokawa K, Kamiyama R. Localization of Fas and Fas ligand in bone marrow cells demonstrating myelodysplasia. Leukemia 1998;12:486–92.
[24] Mahotka C, Kreig T, Kreig A, Wenzel M, Suschek CV, Heydthausen M, et al. Distinct in vivo expression patterns of survivin splice variants in renal cell carcinomas. Int J Cancer 2002;100:30–6.
[25] Mahotka C, Wenzel M, Springer E, Gabbert HE, Gerharz CD. Survivin-ΔEx3 and survivin-2B: two novel splice variants of the apoptosis inhibitor survivin with different antiapoptotic properties. Cancer Res 1999;59:6097–102.
[26] Kitagawa M, Takahashi M, Yamaguchi S, Inoue M, Ogawa S, Hirokawa K, et al. Expression of inducible nitric oxide synthase (NOS) in bone marrow cells of myelodysplastic syndromes. Leukemia 1999;13:699–703.
[27] Sawanobori M, Yamaguchi S, Hasegawa M, Inoue M, Suzuki K, Kamiyama R, et al. Expression of YNF receptors and related signaling molecules in the bone marrow form patients with myelodysplastic syndromes. Leuk Res 2003;27:583–91.
[28] Moriai R, Asanuma K, Kobayashi D, Yajima T, Yagihashi A, Yamada M, et al. Quantitative analysis of the anti-apoptotic gene survivin expression in malignant haematopoietic cells. Anticancer Res 2001;21:595–600.
[29] Paydas S, Tanriverdi K, Yavuz S, Disel U, Sahin B, Burgut R. Survivin and aven: two distinct antiapoptotic signals in acute leukemias. Ann Oncol 2003;14:1045–50.
[30] Kamihira S, Yamada Y, Hirakata Y, Tomonaga M, Sugahara K, Hayashi T, et al. Aberrant expression of caspase cascade regulatory genes in adult T-cell leukaemia: survivin is an important determinant for prognosis. Br J Haematol 2001;114:63–9.
[31] Granziero L, Ghia P, Circosta P, Gottardi D, Strola G, Geuna M, et al. Survivin is expressed on CD40 stimulation and interfaces proliferation and apoptosis in B-cell chronic lymphocytic leukemia. Blood 2001;97:2777–83.
[32] Munzert G, Kirchner D, Stobbe H, Bergmann L, Schmid RM, Döhner H. Tumor necrosis factor receptor-associated factor 1 gene overexpression in B-cell chronic lymphocytic leukemia: analysis of NF-κB/Rel-regulated inhibitors of apoptosis. Blood 2002;100:3749–56.
[33] Vogel LA, Noelle RJ. CD40 and its crucial role as a member of the TNFR family. Semin Immunol 1998;10:435–42.
[34] Fluckinger AC, Rossi JF, Bussel A, Bryon P, Banchereau J, Defance T. Responsiveness of chronic lymphocytic leukemia B cells activated via surface Igs or CD40 to B-cell tropic factors. Blood 1992;80:3173–81.
[35] Modrek B, Lee C. A genetic view of alternative splicing. Nat Genet 2002;30:13–9.
[36] Hoffman WH, Biade S, Zilfou JT, Chen J, Murphy M. Transcriptional repression of the anti-apoptotic *survivin* gene by wild type p53. J Biol Chem 2002;277:3247–57.
[37] Mirza A, McGuirk M, Hockenberry TN, Wu Q, Ashar H, Black S, et al. Human survivin is negatively regulated by wild-type p53 and participates in p53-dependent apoptotic pathway. Oncogene 2002;21:2613–22.

Leptosins isolated from marine fungus *Leptoshaeria* species inhibit DNA topoisomerases I and/or II and induce apoptosis by inactivation of Akt/protein kinase B

Miyako Yanagihara,[1] Noriko Sasaki-Takahashi,[1] Tetsuo Sugahara,[1] Seiko Yamamoto,[1] Masahito Shinomi,[1] Izumi Yamashita,[1] Masashi Hayashida,[1] Banri Yamanoha,[2] Atsushi Numata,[3] Takao Yamori[4] and Toshiwo Andoh[1,5]

Departments of [1]Bioinformatics and [2]Environmental Engineering for Symbiosis, Soka University, 1-236 Tangi-cho, Hachioji, Tokyo 192-8577, Japan, [3]Osaka University of Pharmaceutical Sciences, 4-20-1 Nasahara, Takatsuki, Osaka 569-1094, Japan, and [4]Cancer Chemotherapy Center, Japanese Foundation for Cancer Research, 1-37-1 Kamiikebukuro, Toshima-ku, Tokyo 170-0012, Japan

(Received May 2, 2005/Revised July 31, 2005/2nd Revised August 10, 2005/Accepted August 13, 2005/Online publication November 9, 2005)

DNA topoisomerases (topo) I and II are molecular targets of several potent anticancer agents. Thus, inhibitors of these enzymes are potential candidates or model compounds for anticancer drugs. Leptosins (Leps) F and C, indole derivatives, were isolated from a marine fungus, *Leptoshaeria* sp. as cytotoxic substances. *In vitro* cytotoxic effects of Lep were measured using 3-(4,5-dimethylthiazol-2-yl)-2,5-diphenyltetrazolium bromide-based viability assay. Lep F inhibited the activity of topos I and II, whereas Lep C inhibited topo I *in vitro*. Interestingly both of the compounds were found to be catalytic inhibitors of topo I, as evidenced by the lack of stabilization of reaction intermediate cleavable complex (CC), as camptothecin (CPT) does stabilize. Furthermore, Lep C inhibited the CC stabilization induced by CPT *in vitro*. *In vivo* band depletion analysis demonstrated that Lep C likewise appeared not to stabilize CC, and inhibited CC formation by CPT, indicating that Lep C is also a catalytic inhibitor of topo I *in vivo*. Cell cycle analysis of Lep C-treated cells showed that Lep C appeared to inhibit the progress of cells from G_1 to S phase. Lep C induced apoptosis in RPMI8402 cells, as revealed by the accumulation of cells in sub-G_1 phase, activation of caspase-3 and the nucleosomal degradation of chromosomal DNA. Furthermore, Leps F and C inhibited the Akt pathway, as demonstrated by dose-dependent and time-dependent dephosphorylation of Akt (Ser473). Our study shows that Leps are a group of anticancer chemotherapeutic agents with single or dual catalytic inhibitory activities against topos I and II. (*Cancer Sci* 2005; 96: 816–824)

DNA topoisomerases (topos) are essential nuclear enzymes that regulate DNA topology. There are two classes of topos, classes I and II, that differ in their function and mechanism of action.[1–4] Class I enzymes (topo I, EC 5.99.1.2) act by making a transient break in one DNA strand, allowing the DNA to swivel and release torsional strain, changing the linking number by steps of one.[2,4] Class II enzymes (topo II, EC 5.99.1.3) make transient breaks in both strands of one DNA molecule, allowing the passage of another DNA duplex through the gap, changing the linking number by steps of two.[1–3] These enzymes are crucial for cellular genetic processes such as DNA replication, transcription, recombination, and chromosome segregation at mitosis.

It has long been accepted that topos are valuable targets of cancer chemotherapeutics.[2–5] Several classes of topo inhibitors have been introduced into cancer clinics as potent anticancer drugs, including camptothecin (CPT) derivatives (e.g. irinotecan and topotecan) inhibiting topo I[4] and anthracyclines (e.g. doxorubicin and mitoxantorone), epipodophyllotoxins (e.g. etoposide [VP-16], aminoacridines (e.g. m-AMSA) and ellipticines targeting topo II.[4,5] These agents are active in both hematological and solid malignancies. The activity of these agents is thought to result from stabilization of the DNA/topo cleavable complex (CC), an intermediate in the catalytic cycle of the enzymes,[2,5,6] resulting ultimately in apoptosis. A number of new topo inhibitors have recently been reported that do not stabilize CC. Thus, two general mechanistic classes of topo inhibitors, especially for topo II, have recently been described:[7] (1) classical topo 'poisons' that stabilize CC and stimulate single- or double-strand cleavage of DNA, such as CPT and its derivatives, indolocarbazoles for topo I, and TAS-103[8] for topos I and II; and (2) catalytic inhibitors that prevent the catalytic cycle of the enzymes at steps other than cleavage intermediates, such as dioxopiperazines, ICRF-193 and ICRF-154,[7,9,10] aclarubicin,[11] intoplicin,[12] and F11782.[13] Some of these compounds are dual inhibitors of topos I and II. The catalytic inhibitors of topo II, merbarone[14,15] and dioxopiperazines,[9,10] have been extensively studied and have been shown to inhibit the reopening of the closed clamp formed by the enzyme around DNA by inhibiting the ATPase activity of the enzyme, thus sequestering the enzyme within the cell.[7,16,17]

[5]To whom correspondence should be addressed. E-mail: andoh@t.soka.ac.jp
Abbreviations: CC, cleavable complex; CPT, camptothecin; DEVD-AMC, acetyl-L-aspartyl-L-glutamyl-L-valyl-L-aspartyl-7-amino-4-methyl-coumarin; DMSO, dimethylsulfoxide; DTT, dithiothreitol; kDNA, kinetoplast DNA; Lep, leptosin; MTT, 3-(4,5-dimethylthiazol-2-yl)-2,5-diphenyltetrazolium bromide; PBS, phosphate-buffered saline; PI3-K, phosphatidylinositol-3-kinase; SDS, sodium dodecylsulfate; topo, DNA topoisomerase; VP-16, etoposide.

doi: 10.1111/j.1349-7006.2005.00117.x

Leptosin (Lep) derivatives, Lep F and Lep C, have been isolated in our laboratory in search of cytotoxic compounds.[18] In this report we describe that both of the compounds exhibited biological activities, such as the inhibition of topos and cytotoxicity against various tumor cells. Leps are strong catalytic inhibitors of topos, Lep C inhibiting topo I and Lep F inhibiting both topos I and II *in vitro*; Lep C targets topo I *in vivo* as well. These compounds have strong growth-inhibiting and apoptosis-inducing activities against human lymphoblastoid RPMI8402 cells and human embryonic kidney cell line 293 cells. Leps F and C inhibit the survival pathway by inactivation (i.e. dephosphorylation) of Akt/protein kinase B (EC 2.7.1.37).

Materials and Methods

Drugs and chemicals

Leps F and C (Fig. 1) were isolated from a marine fungus *Lestoshaeria* sp.[18] CPT was provided by Yakult Honsha (Tokyo, Japan). VP-16 was provided by Bristol-Myers Squibb (Brea, CA, USA). ICRF-193 was obtained from Zenyaku Kogyo (Tokyo, Japan).

Preparation and assay of topos

Recombinant human topo IIα was purified from a baculovirus expression system as described elsewhere.[19] One unit of topo IIα was defined as the minimal amount of activity required to decatenate 0.2 μg of kinetoplast DNA (kDNA). Isolation of murine topo I from Ehrlich ascites tumor cells was carried out essentially as described previously,[20] except that salt extraction of the enzyme from nuclei was with 0.35 M NaCl and the hydroxyapatite column chromatography was skipped. Topo I activity was monitored by relaxation of supercoiled plasmid DNA.[20,21] One unit of topo I was defined as the minimal amount of activity required to relax 0.2 μg of pT2GN plasmid DNA.

Preparation of kDNA

kDNA was isolated from protozoa *Crithidia fasciculata* as described previously[19,22,23] with some modifications.

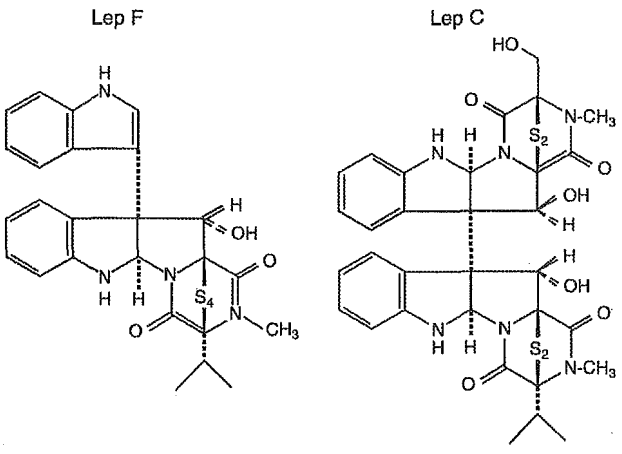

Fig. 1. Chemical structures of Lep F and C.

Inhibitory effect of test compounds on topo II activity was evaluated by detecting the conversion of catenated kDNA to monomer minicircles as described previously.[19,24]

Topo I-mediated DNA cleavage assay

Topo I-mediated cleavable complex formation assay was carried out as described elsewhere[21,25,26] with some modifications. The reaction mixture (20 μL) contained 50 mM Tris-HCl, pH 8.0, 50 mM NaCl, 0.5 mM dithiothreitol (DTT), 10% glycerol, 30 μg/mL bovine serum albumin, 10 units of topo I, 0.2 μg of supercoiled pT2GN plasmid DNA and 1 μL of a solution of Leps or CPT as a positive control. Reaction mixtures were incubated for 15 min at 37°C. In experiments of drug combinations, 1 μL each of a test compound and CPT were sequentially added, one before the first incubation at 37°C for 15 min, followed by a further 30-min incubation after the addition of the other, as described in the legend to Figure 3. Then 2.5 μL of 10% sodium dodecylsulfate (SDS) and 2 μL of 20 mg/mL proteinase K were added and the reaction mixtures were digested at 37°C for 1 h. Denatured proteins and drugs were removed by extraction with 1 : 1 mixture of phenol/chloroform. Aqueous phases were taken and mixed with 4 μL of the dye/SDS stop solution and analyzed by electrophoresis on 0.6% agarose gels in the presence of 0.1 μg/mL of ethidium bromide.

Cell culture

Human lymphoblastoid RPMI8402 cells were cultured in RPMI-1640 medium containing 10% fetal bovine serum. Human embryonic kidney cell line 293 cells were cultured in Dulbecco's modified Eagle's medium containing 10% fetal bovine serum. Both of these cell cultures were kept at 37°C in a humidified 5% CO_2 incubator.

Band depletion assay

RPMI8402 cells (2×10^5) in 200 μL of RPMI-1640 medium were prepared in a microcentrifuge tube, treated with each drug or a combination of Lep C and CPT at concentrations described in Figure 4a, and incubated for 15 min at 37°C. For a negative control, we treated cells with 2 μL of dimethylsulfoxide (DMSO) at the same time. Cells were harvested by centrifugation and resuspended in a 10 μL of phosphate-buffered saline (PBS) spiked with two-fold concentrations of the topo inhibitors, as described, to avoid rapid dissolution of the CC. Five μL of 4 × SDS sample buffer (250 mM Tris-HCl, pH 6.8, 8% SDS, 2.8 mM 2-mercaptoethanol, 40% glycerol, 0.008% bromophenol blue) was added and immediately sonicated with Sonifier 450 (Branson Ultrasonics, Danbury, CT, USA) to diminish viscosity. Samples were loaded onto 8% SDS polyacrylamide gels, electrophoresed and blotted onto a nitrocellulose membrane. Topo I was detected by antitopo I Scl70 human serum. The membrane was stained with Ponsau S (Sigma, St Louis, MO, USA) according to the manufacturer's instructions.

Drug sensitivity assay of cancer cells

RPMI8402 cells were plated in 96-well plates at an initial density of 2000 cells/well in culture medium. One day after plating, cells were treated with various concentrations of chemotherapeutic agents and cell survival was estimated

by the 3-(4,5-dimethylthiazol-2-yl)-2,5-diphenyltetrazolium bromide (MTT) method.[27] Three days after the drug treatment plates were centrifuged, the medium was removed and 200 μL of fresh medium containing 250 μg/mL MTT (Sigma) solution was added to each well and incubated at 37°C for 4 h. The plates were centrifuged again, the supernatant was removed and precipitates were dissolved in 150 μL DMSO. The absorbance at 570 nm was measured for each well using a microplate reader (Bio-Rad; Hercules, CA, USA). The IC_{50} values of drugs were calculated from the survival of cells treated for 3 days. IC_{50} was defined as the concentration of drug causing 50% inhibition of cell growth, as compared with the solvent control.

For drug combination analysis, pretreatment of RPMI8402 cells was performed by the addition of Lep C to the cells at various concentrations as indicated. Ten minutes later 20 nM of CPT was added to the culture and incubated for 1 h at 37°C. Then the cells were harvested, washed with PBS and reseeded in 96-well plates at a density of 2000 cells/well. Two days after reseeding, cell survival was estimated by the MTT method.

Cell cycle distribution analysis of cells treated with Lep C

RPMI8402 cells were seeded in 100 mm dishes at an initial density of 5×10^6 cells/dish in culture medium. Twelve hours after plating, the cells were treated with various concentrations of Lep C and other chemotherapeutic agents as indicated. Twenty-four hours after the drug treatment, the cells were fixed with ice-cold 70% ethanol for 30 min, resuspended in 10 μg/mL DNase-free RNase A and 10 μg/mL propidium iodide, and incubated for 30 min at room temperature. After filtration with a nylon cell strainer, cell cycle distribution was monitored with an EPICS Elite (Beckman Coulter, Fullerton, CA, USA).

Caspase assay

Cells were lyzed in caspase lysis buffer (1 mM HEPES, pH 7.4, 2 mM EDTA, 0.1% CHAPS and 5 mM DTT) and protein concentrations measured by Bio-Rad reagent. Forty micrograms of proteins of cell lysate were incubated with 20 μM acetyl-L-aspartyl-L-glutamyl-L-valyl-L-aspartyl-7-amino-4-methylcoumarin (DEVD-AMC; Peptide Institute, Osaka, Japan) in caspase assay buffer (20 mM HEPES, pH 7.4, 10% glycerol and 2 mM DTT) for 60 min at 37°C. AMC released was measured by Fluoroscan Acent FL (Thermo Labsystems, Helsinki, Finland).

DNA ladder formation analysis

Cells (3×10^6) were washed once with PBS, resuspended in lysis buffer (20 mM Tris-HCl, pH 7.5, 10 mM EDTA, 0.5% Triton X-100) and centrifuged 12 000 *g* for 5 min at 4°C. The supernatant was then treated with 0.2 mg/mL RNase for 1 h at 37°C, followed by treatment with 0.4 mg/mL proteinase K for 30 min at 50°C. The mixture was added with 20 μL of 5 M NaCl and 120 μL of isopropanol and stood overnight at −20°C. After centrifugation at 12 000 *g* at 4°C for 5 min, precipitate was dissolved in 20 μL of TE buffer (10 mM Tris-HCl, pH 7.4, 1 mM EDTA) added with 4 μL of 6× loading dye (50% glycerol, 0.1% bromophenol blue), and electrophoresed on 2% agarose gels containing 0.1 μg/mL ethidium bromide.

Western blot analysis

Cells were solubilized with RIPA buffer (25 mM Tris-HCl, pH 8.0, 150 mM NaCl, 0.1% SDS, 0.5% sodium deoxycholate, 1% NP-40, 10% glycerol, 2 mM EDTA).[28] The cell lysates were then subjected to 10% SDS-polyacrylamide gel electrophoresis. The proteins were transblotted onto a nitrocellulose membrane. After blocking, the membranes were incubated with anti-Akt or antiphospho-Akt (Ser473) antibodies (Cell Signaling Technology, Beverly, MA, USA). The membrane was then incubated with an appropriate peroxidase-conjugated secondary antibody and developed with the enhanced chemiluminescence mixture (Amersham Bioscience, Piscataway, NJ, USA).

Results

Lep C inhibits topo I but Lep F inhibits both topo I and II *in vitro*

We tested Leps for inhibition of topo I activity by monitoring the relaxation of supercoiled plasmid DNA, and for inhibition of topo II activity by kDNA decatination assay as described earlier.[19] Both compounds strongly inhibited topo I activity, with IC_{50} values of between 3 and 10 μM for Leps C and F (Fig. 2a). However, inhibition of topo II activity was only observed with Lep F with an IC_{50} value of 10–30 μM. The IC_{50} for Lep C was more than 100 μM (Fig. 2b).

Inhibition of topo I by Leps C and F does not involve significant accumulation of DNA strand breaks

Topo inhibitors are classified according to whether they induce an accumulation of topo-dependent DNA strand breaks as CC or not, reflecting the mechanism of inhibition. We examined whether Leps C and F inhibiting topo I induced

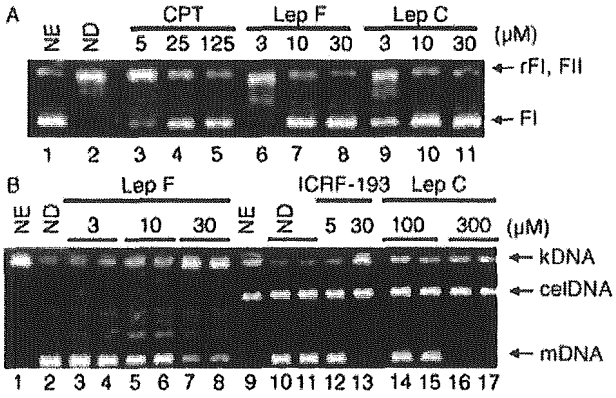

Fig. 2. Inhibition of DNA topoisomerase I (a) and II (b) by Leps F and C. (a) Lane 1, no enzyme (NE) added to the reaction mixture; lane 2, no test compounds (no drugs, ND) were included in the reaction; lane 3, 5 μM CPT; lane 4, 25 μM CPT; lane 5, 125 μM CPT; lane 6, 3 μM Lep F; lane 7, 10 μM Lep F; lane 8, 30 μM Lep F; lane 9, 3 μM Lep C; lane 10, 10 μM Lep C; lane 11, 30 μM Lep C. FI, supercoiled form I; FII, nicked circular form II; rFI, relaxed form I. (b) Lane 1, NE; lane 2, ND; lanes 3 and 4, 3 μM Lep F; lanes 5 and 6, 10 μM Lep F; lanes 7 and 8, 30 μM Lep F; lane 9, NE; lanes 10 and 11, ND; lane 12, 5 μM ICRF-193; lane 13, 30 μM ICRF-193; lanes 14 and 15, 100 μM Lep C; lanes 16 and 17, 300 μM Lep C. celDNA, cellular DNA; kDNA, kinetoplast DNA; mDNA, monomer circular DNA.

 doi: 10.1111/j.1349-7006.2005.0117.x

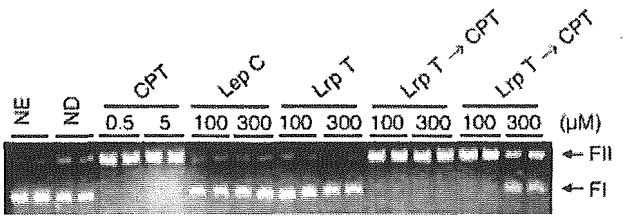

Fig. 3. Inhibition by Lep derivatives of topo I-mediated DNA cleavage induced by CPT. Reaction mixtures containing substrate DNAs and topo I were incubated in the presence of test compounds as described in Figure 2 and under Materials and Methods. Supercoiled FI plasmid DNA was used as the substrate. After the reaction enzyme and test compounds were inactivated, the reaction products were electrophoresed on 0.6% agarose gels.

an accumulation of CC, as described in Materials and Methods. As shown in Figure 3, CPT, a typical topo I poison, induced the accumulation of CC as indicated by an increase in nicked circular form II DNA (FII). No accumulation of FII was observed with Leps C and F up to 300 μM, indicating that Lep is not a poison but a catalytic inhibitor of topo I. It is of great interest to note that Lep C partially inhibited the CC formation by CPT, as illustrated in the two far-right lanes in Figure 3, suggesting that Lep C suppresses the stabilization of CC induced by CPT and that Lep C interacted with topo I in steps other than those of CC formation.

Lep C targets topo I in cultured cells

To quantify DNA–topo CC formed within drug-treated cells, the band depletion assay was employed according to previous reports,[19,29,30] with some modifications. Treatment of human lymphoblastoid RPMI8402 cells with the topo I poison CPT resulted in the depletion of free enzymes detected by Western blotting (Fig. 4a), suggesting the accumulation of topo I-mediated CC within the cells. In contrast, treatment of cells with Lep C, used as a representative Lep with higher potency

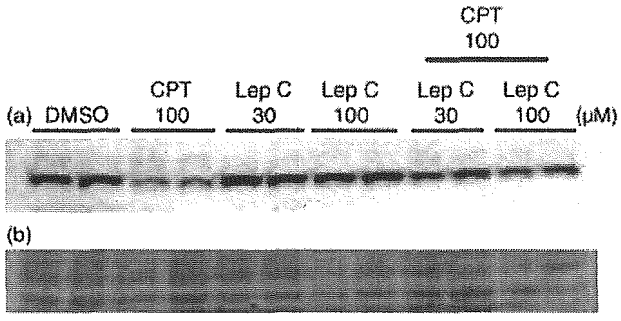

Fig. 4. Band depletion analysis of topo I in RPMI8402 human lymphoblastoma cells. (a) Cells were exposed to drugs singly or in combination, as described under Materials and Methods. Fifteen minutes after incubation, cells were collected by centrifugation and lyzed by addition of SDS-containing lysis buffer, followed by sonication. After protein determination, immunoblotting was performed. (b) It was confirmed by staining the membrane with Ponsau S that the amounts of proteins loaded on the gel were very similar.

of topo I inhibition, did not deplete free enzymes, indicating that Lep C is not a poison like CPT. Treatment of the cells with Lep C prior to CPT tended to restore the free topo I level, as compared with CPT alone, suggesting that Lep C competes with CPT for topo I *in vivo*. This competitive interaction of the two drugs *in vivo* appears to mimic the result obtained in *in vitro* study (Fig. 3). The amount of proteins loaded in each of the lanes of the gel was nearly the same, as shown in Figure 4b.

Lep derivatives inhibit the growth of RPMI8402 cells

The cytotoxicity of Lep C, Lep F, CPT and VP-16 were evaluated with RPMI8402 cells. Dose–response curves were obtained and IC_{50} values were calculated, as shown in Figure 5. The potency of the drugs was in the following order: Lep C > CPT > Lep F > VP-16, as depicted in the figure. RPMI8402 cells exhibited higher sensitivity to Lep derivatives than VP-16 and were nearly as sensitive to Leps as CPT. Examination of the toxicity of Leps F and C on 39 human cancer cell lines established from various tissues from the Cancer Chemotherapy Center, Japanese Foundation for Cancer Research, Tokyo, Japan,[31] revealed a similar level of cytotoxicity, with MG-MID (mean logarithm of GI_{50} values, 50% growth-inhibitory concentrations) of –7.41 and –6.8 for Lep C and Lep F, respectively.

Leps F and C induce apoptosis in RPMI8402 cells

The sensitivity of mammalian cells against CPT cytotoxicity was shown to be the largest in S phase of the cell cycle, or rather it was S-phase-specific,[32–34] so it is of great interest to investigate which cell cycle phase Leps might affect. Analysis of cell cycle distribution of cells treated with Lep C by flow cytometry showed that, compared with the solvent control (Fig. 6a), cells treated with Lep C appeared to be

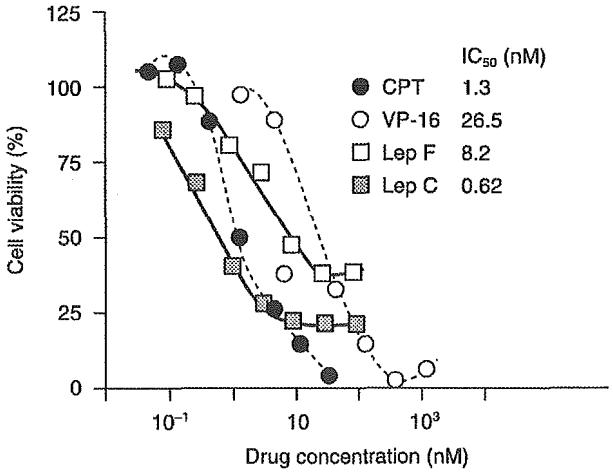

Fig. 5. Cytotoxic activity of Lep derivatives. RPMI8402 human lymphoblastoma cells in 96-well plates were treated with various concentrations of chemotherapeutic agents and cell survival was estimated by the MTT method. The IC_{50} values of drugs were calculated from the survival of cells treated for 3 days. IC_{50} was defined as the concentration of drug causing 50% inhibition of cell growth, as compared with the solvent control DMSO.

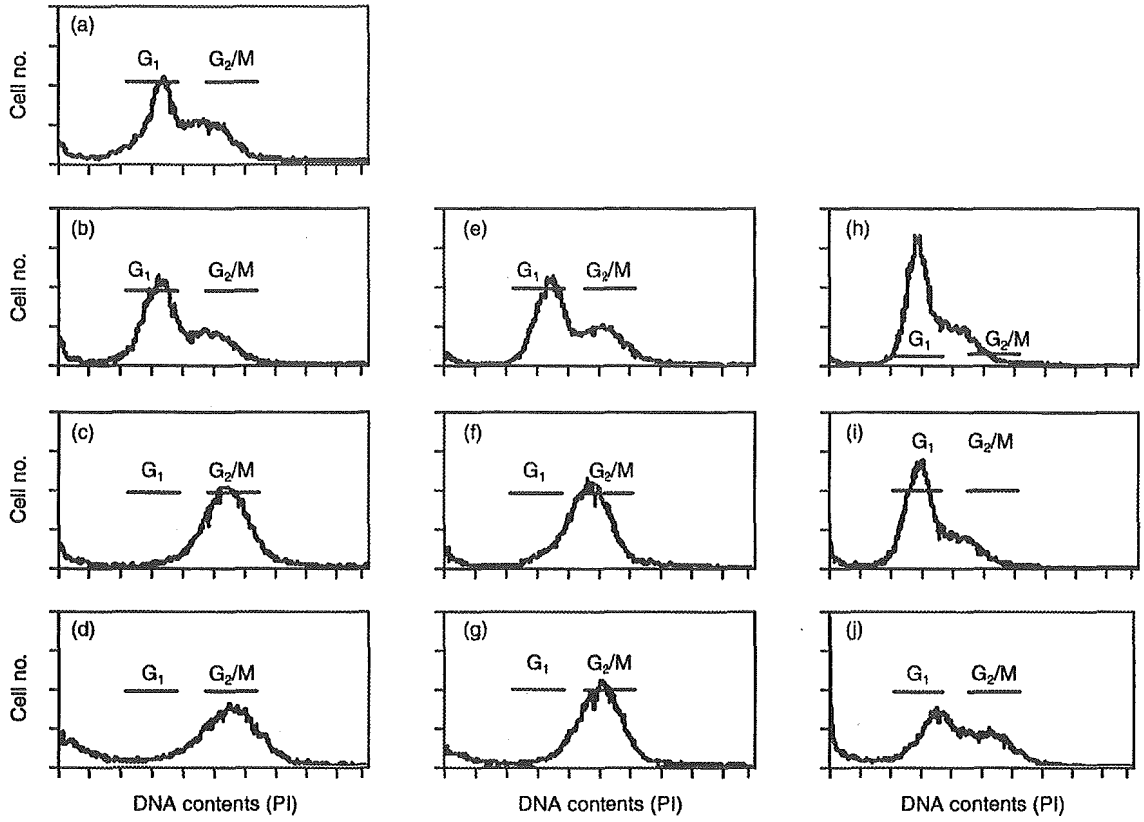

Fig. 6. Cell cycle distribution of cells treated with Lep C. RPMI8402 human lymphoblastoma cells were treated with various concentrations of chemotherapeutic agents for 24 h and flow cytometric analysis was performed, as described in Materials and Methods. (a) solvent control DMSO; (b) 0.02 μM CPT; (c) 0.06 μM CPT; (d) 0.18 μM CPT; (e) 0.3 μM VP-16; (f) 1.0 μM VP-16; (g) 3.0 μM VP-16; (h) 3 nM Lep C; (i) 10 nM Lep C; (j) 30 nM Lep C.

arrested in G_1 phase, as the G_1 cell population increased as the drug concentration was increased up to 10 nM (Fig. 6h,i). However, when the Lep C concentration was increased to 30 nM, the G_1 population decreased and conversely the sub-G_1 fraction increased, indicating that apoptosis took place in high concentrations of the drug. In contrast, cells treated with topo I poison CPT appeared to be arrested in late S to G_2/M phase (Fig. 6b–d). A similar trend of the effect of topo II poison VP-16 arresting cells at late S to G_2/M phase was observed. These experiments clearly indicate that the cellular effects of topo poisons and putative catalytic inhibitors may be different.

We also measured caspase-3 activation as a criterion of apoptosis in Lep-treated RPMI8402 cells using a fluorometric assay, using DEVD-AMC as a substrate. Caspase-3 activity increased after 6 h of treatment with each concentration of drugs (Fig. 7). CPT induced caspase activation maximally at 1 μM. Lep C appears to be stronger than Lep F in caspase activation, as the activity increases dose-dependently with Lep F up to 100 μM, whereas maximum activity was obtained by Lep C at 10 μM. Next, we analyzed DNA strand breaks in Lep-treated RPMI8402 cells. DNA ladder formation indicative of nucleosome-level degradation of DNA, and characteristic of apoptosis, was observed at 6 h after addition of the

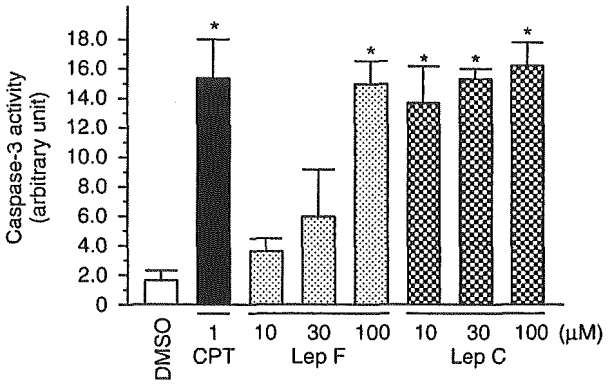

Fig. 7. Activation of caspase-3 by Lep treatment in RPMI8402 human lymphoblastoma cells. Cells were treated with the indicated concentrations of Lep for 6 h. Cell lysates were incubated with the fluorogenic tetrapeptide DEVD-AMC (20 μM) for 1 h at 37°C. The increase in caspase-3 activity in the cell lysates was determined as described in Materials and Methods. The vertical bars represent the standard deviation value of triplicate determinations. Asterisks indicate significant differences from that of the solvent control with *P*-values lower than 0.01.

 doi: 10.1111/j.1349-7006.2005.0117.x